45

RECENT RESEARCH CONTRIBUTIONS ON THE SOUTH ASIAN MONSOON

T.N. Krishnamurti, Vasubandhu Misra, Bhaskar Jha and Mukul Tewari

INTRODUCTION

This review of monsoon research emphasizes mostly the contributions during recent decades. Research covering periods prior to that have been reviewed in a number of publications: for example, Ramage (1971), Krishnamurti (1978), Chang and Krishnamurti (1987), Rao (1976), Asnani (1993) and several others. These past reviews have covered issues such as the annual cycle of the monsoon; the onset, active and break monsoons; the diurnal change; monsoon depressions, their structure and motion characteristics; large-scale heat sources and sinks; quasi-biweekly oscillations; intraseasonal oscillations on the time scale of 30 to 50 days; winter monsoon cold surges over the South China Sea; surge vortices; onset of the Australian monsoon; the equatorial and monsoonal westerly wind bursts; and the Maiu fronts along the south China coast. In recent years the emphasis on monsoon research has shifted to intraseasonal and interannual variability of the monsoon. Observational studies have examined the issues of precipitation, droughts and floods on different time scales ranging from a couple of weeks to several years. There is a large interest in the effects of El Niño (warm phase of the Southern Oscillation) time scale variability. Here the effects of sea surface temperature anomalies and the snow cover (and depth) over the Himalayas, Central Asia and Western Siberia on the monsoon have drawn considerable interest. The issues of intraseasonal time scale variabilities in the upper troposphere and lower stratosphere of polar latitudes (near 60° and 70°) are now being related to the meridional propagation of wave energy flux from the tropics. This required a non-linear theory (and modeling) of the wave energy flux from the monsoon latitudes across the so-called critical latitudes. Other majot advances have occurred in the climate modeling of the monsoon where more questions are being raised in reference to the ultimate role of the lower boundary conditions (the sea surface temperatures and the snow cover). It is felt that large internal variability of the monsoon may make it very difficult to carry out meaningful forecasts of the monsoon on the intraseasonal and interannual time scales.

High resolution simulations (on the medium-range time scale) have shown that the prediction of monsoons may require the prediction of their organization of convection. This review includes a detailed discussion on that topic, which in turn raises some interesting possibilities for future climate modeling of the monsoon. These earlier reviews also covered issues on the early numerical weather prediction and climate modeling efforts. In this present review we shall address recent progress in several areas of monsoon research such as: numerical weather prediction, effects of dust aerosols, intraseasonal and interannual variability, winter monsoon phenomena, and the cooling of the Arabian sea during the monsoon season.

SOME ONSET FEATURES

The onset of monsoon occurs during the early part of May over Burma and the south China coast, and during early June over southwestern India. In this section we present some recent findings related to the onset issues. Very rapid cooling of the Arabian Sea (far east of the regions of coastal upwelling) is obsetved soon after the onset of the strong southwesterly monsoonal

winds. This evolution of cooling is somewhat similar to that seen in the wake of hurricanes. Typically, the onset of the Indian summer monsoon is characterized by a tropical storm which is normally called the onset vortex. Figures 45.1a, b, c and d, based on Krishnamurti *et al.* (1979), illustrate the time variability of the winds and sea surface temperature during the Global Atmospheric Research Project (GARP) Monsoon Experiment (1979) over two different ship locations at 9°N, 67°E and 7°N, 69°E, respectively. It is apparent from these figures, that in a matter of two days after the onset of strong winds around June 11, 1979, the sea surface temperature dropped by about 3 degrees. This period of onset featured a tropical storm with winds as large as 60 knots (Krishnamurti *et al.* 1979). Krishnamurti *et al.* (1979) computed the curl of the wind stress from the time of the onset of strong winds. Figures 45.2a and b show the latitude–time sections of the zonally averaged (between 55°E and 70°E) curl of the wind stress, and sea surface temperature. It is striking to note in these figures that the axis of cold SSTs coincides with the axis of the strongest positive wind stress curl suggesting wind stress induced upwelling of the mid-ocean, and the importance of the oceanic mixed layer.

The mixed layer depth over the Arabian Sea and the Indian Ocean has been studied extensively by the Atlantic Oceanography and Meteorology Laboratory at Miami for many years. Figures 45.3a, b and c illustrate the climatological mixed layer depth for January, March and July, from their compilations. These show the response to the wind, i.e. from the reverse Somali jet in January, the northward moving wind gyre in March, and the full-fledged summer monsoon flows of July. (The Somali jet is a summertime phenomenon that is seen with maximum winds at the 1 km level above sea level along the east African coast. That jet exits Africa near Somalia on a westerly jet. A reverse situation is seen during the northern winter where the low-level jet is somewhat weaker and follows a

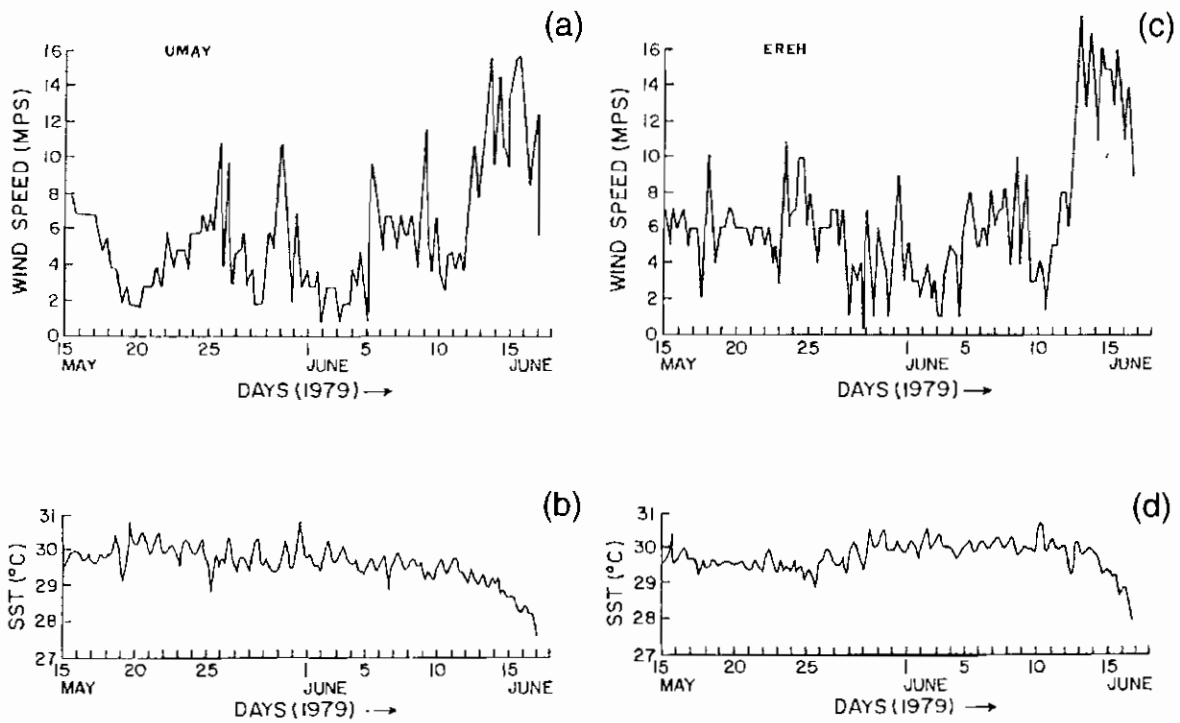

Figure 45.1 Variability of the wind and SST during GARP monsoon experiment (1979) over two different ship locations at 9°N, 67°E, and 7°N, 69°E, respectively

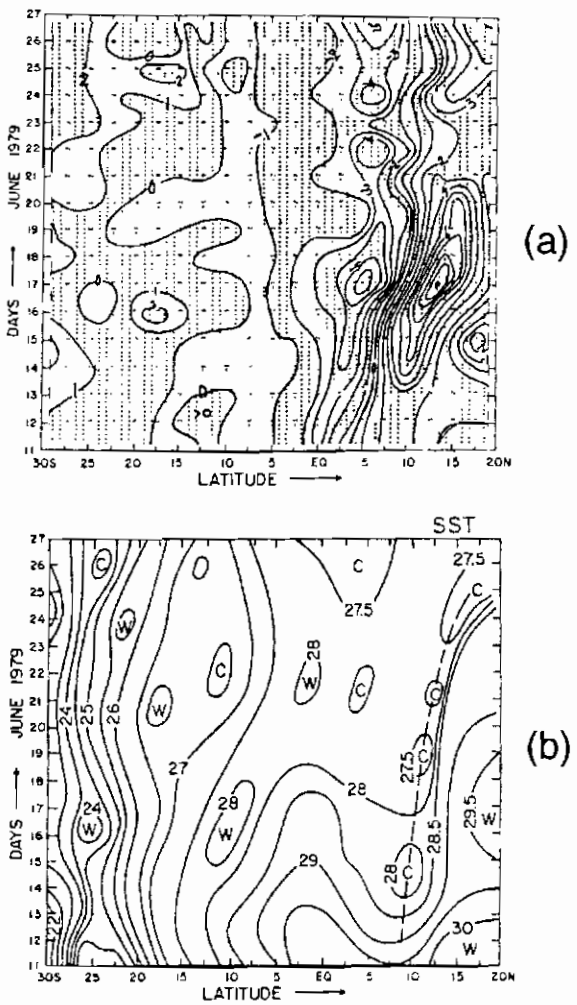

Figure 45.2 Latitude–time sections of zonally averaged (between 55°E and 70°E) curl of wind stress and SST

somewhat reverse track and hence the name, reverse Somali jet.) These distributions and their variations are important for the validation of coupled atmospheric ocean models.

Joshi *et al.* (1990) noted a spectacular rise in the 300 mb (9 km) temperatures over the western, central and eastern Tibetan Plateau and over the region of the heat low over Pakistan. They noted a spectacular rise at 300 mb commencing almost two weeks prior to the onset of monsoon rains over southwestern India (Figure 45.4). This analysis suggests that a mean 300 mb temperature over these regions of around 243K could be used as a threshold for the onset of the Indian monsoon. These results are consistent with the previous studies of Krishnamurti and Ramanathan (1982) on the response of the onset of monsoon to differential heating. This appears to be an important parameter for monitoring the onset of monsoons.

An important issue of offshore rainfall over the Arabian Sea during the active summer monsoon phase has been investigated by several scientists in recent years; for example, Grossman and Duran (1984), Smith and Lin (1983), and Ogura and Yoshizaki (1988). Among these, Ogura's study includes dynamical, orographic and the effects of cumulus convection. According to this study, the upper tropospheric easterlies tend to maintain the convection offshore. This convection is initiated over regions of strong moisture flux over the Arabian Sea where the southwesterly monsoon flow undergoes a slow offshore ascent well before reaching the slopes of the western Ghats. The orography of the western Ghats is still quite important in providing the slow offshore ascent. The same kinds of features of monsoon convection, during late May, have been noted offshore of the Burmese Mountains over the eastern Bay of Bengal. The offshore convection is an important aspect of the onset of monsoons over India and Burma.

Near the Somali coast, over Garissa in northern Kenya, observations of the wind show a pronounced diurnal change from roughly 12 m s^{-1} to 24 m s^{-1} between afternoon hours and the early morning hours. Figure 45.5 illustrates these features. A detailed study of similar observations has also been presented by Cadet (1983). The Mascarene high and the Monsoon trough over northeast India are two of the major elements of the summer monsoon. The pressure difference between the Mascarene high and the monsoon trough is in fact a measure of the differential heating that drives the monsoon. That forcing of the monsoon can be measured by the kinetic energy of the 850 mb (1.5 km) winds over the central Arabian Sea. Figure 45.6 illustrates a season-long behavior of these two parameters. This illustration clearly shows a strong relationship among the pressure difference between the Mascarene high and the monsoon trough (ΔP) and the kinetic energy (KE) of the Arabian Sea winds. This strong relationship among ΔP and

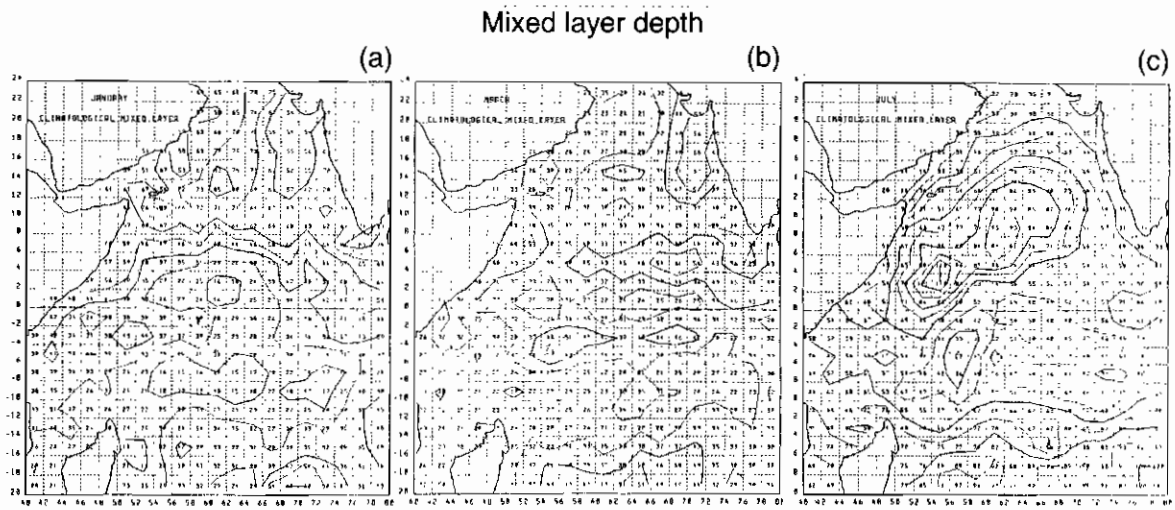

Figure 45.3 Climatological mixed layer depth for (a) January, (b) March and (c) July

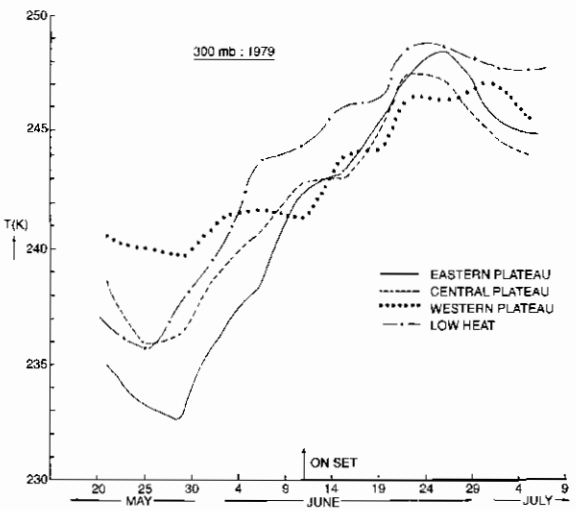

Figure 45.4 The temperature changes at 300 mb level over the heat low, and the three plateau regions during May through July 1979. (From Joshi *et al.* 1990)

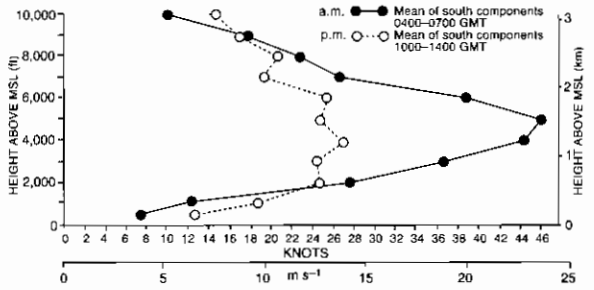

Figure 45.5 Mean diurnal changes in the low-level jet stream system at Garissa, Kenya, during a two-month period (June, July, 1973) of stronger than normal cross-equatorial flow. (From Anderson 1981)

KE should be used by modelers aiming to simulate the wet and dry spells of the monsoon over an entire season.

It may be of interest to examine the time history of all of these variables during an entire monsoon season. We have been limited in our review in this regard due to the absence of detailed observations.

DUST AEROSOLS EFFECT ON THE SYNOPTIC-SCALE MONSOON DISTRIBUTIONS

The heat low over the Arabian Peninsula is characterized by a well-mixed layer between the surface and 800 mb (2 km). An outflow layer exists at around 750 mb (2.5 km). The air above 750 mb generally displays descending motions accompanied by upper tropospheric convergence over the heat low near 200 mb (12 km). The maintenance of the thermal stratification, despite the net radiative heat loss, pointed out by Charney (1975), is aided by dry

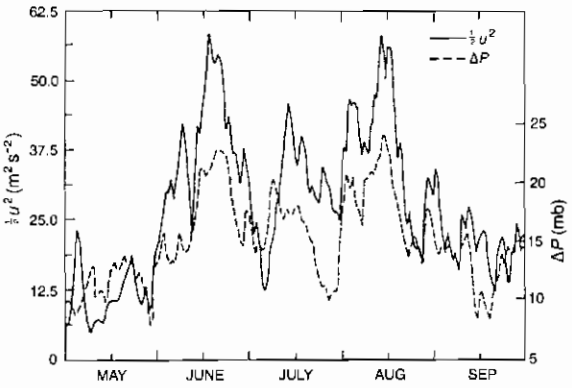

Figure 45.6 Mean zonal kinetic energy over the Arabian Sea over the domain (1.25°S to 13.75°N and 51.25°E to 71.25°E) and pressure difference between the Mascarene high and the monsoon trough as a function of time. (From Cadet 1983)

convection, radiation in the mixed layer and by subsidence in the upper troposphere. The heat budget studies over the region suggest a continual import of energy through upper tropospheric circulations from neighboring convective areas, especially the Indian summer monsoon.

The Saudi Arabian region is exposed to extensive dust aerosols in the summer especially during the months of June and July. This dusty condition arises on account of strong winds in the lower troposphere which inject dust aerosols and cause a high turbidity in the region. In order to calculate the radiative heating due to dust aerosols, it is required that aerosol properties such as optical depth (τ), single-scattering albedo (defined as the ratio of the scattered radiation to the total radiation) ($\tilde{\omega}$) and asymmetry factor (a measure of deviation of scattered radiation around a scattering partical from its mean value) (g), as well as their space and time variations, are known. (Optical depth is the depth of an absorbing layer as felt by atmospheric radiation. It is obtained by a vertical integration of the absorbing constituent through the depth of study. This depth does have atmospheric dependence on temperature and pressure generally.) These parameters depend upon the dust aerosol characteristics like aerosol density and size distribution and their refraction index, which can be determined from field experiments. In recent years, many experimental studies have been conducted to assess the properties of dust aerosols. These include the GARP Atlantic Tropical Experiment over West Africa and the Atlantic Ocean, the 1987 USSR–USA dust aerosol experiment over central Asia in Tadzhikistan, and the aircraft measurements of dust aerosols over Saudi Arabia and adjacent regions during the summer Monsoon Experiment (MONEX) 1979. The studies, based on the Mei scattering theory (scattering of radiation by particles whose size is comparable to or greater than the wavelength of radiation), and utilizing data obtained from these experiments have provided some knowledge on the optical properties of dust aerosols (Patterson *et al.* 1977; Carlson and Benjamin 1980; d'Almeida 1987; Ackerman and Chung 1992).

The dust aerosol properties documented by d'Almeida (1987) and Ackerman and Chung (1992), based on measurements over Saudi Arabia during summer MONEX, show that the single-scattering albedo and asymmetry factor are constant with height within the measurement errors. During a duststorm, Levin *et al.* (1980) obtained the optical depth (τ) of dust layer over the spectral bands 0.70 μm, 0.55 μm and 0.40 μm as 3.56, 3.17 and 2.87, respectively. This is in agreement with d'Almeida (1987), who observed τ to be in the range of 2.8 to 3.5 during duststorm conditions. In moderate and light dust conditions the optical depth was in the range of 1.0–2.5 and 0.4–0.5, respectively.

The three categories of atmospheric dustiness (i.e. light, moderate or heavy) and the dust optical properties classified in terms of the horizontal visibility range based on a long-term study by d'Almeida (1987) are as follows:

1 A visibility range higher than 7 km is light dust.
2 Visibility ranges between 2 km and 7 km are termed moderate dust.
3 Visibility ranges lower than 2 km are termed sandstorm.

The optical properties for these three categories of dust aerosol given by d'Almeida (1987) and used in this study are summarized in Table 45.1 for the spectral bands 0.40 μm, 0.55 μm and 0.77 μm.

The following observations of Akerman and Cox (1982), using research aircraft-based direct measurements of short- and long-wave irradiances over the Saudi Arabian desert and over the northern Arabian

Table 45.1 Dust aerosol radiative characteristics

Dust category	*Wavelength (μm)*	*Extinction coefficient (km^{-1})*	*Single scattering albedo*	*Asymmetry factor*
Light dust	0.40	0.224	0.751	0.791
	0.55	0.229	0.791	0.773
	0.70	0.230	0.825	0.757
Moderate dust	0.40	0.945	0.706	0.841
	0.55	0.949	0.750	0.838
	0.70	0.956	0.718	0.845
Heavy dust	0.40	2.182	0.737	0.793
	0.55	2.232	0.777	0.778
	0.70	2.255	0.817	0.763

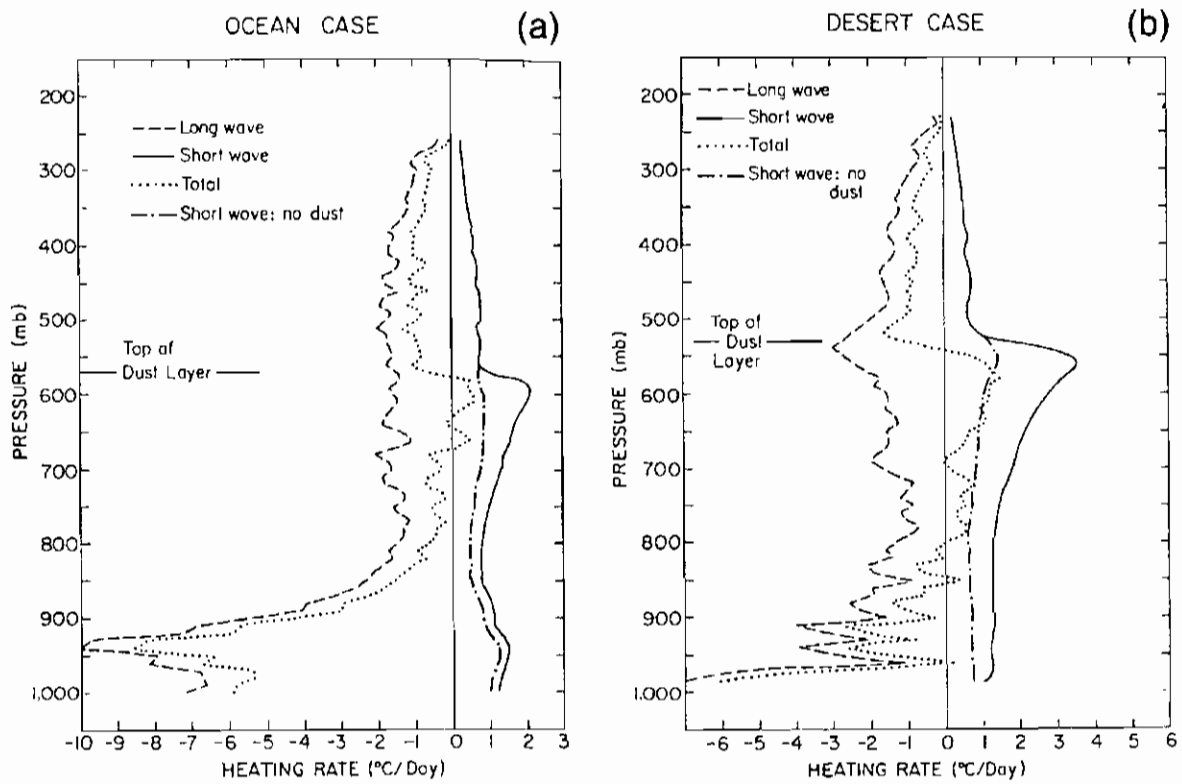

Figure 45.7 (a) The 24-hr mean radiative heating rates over the Arabian Sea. (b) The 24-hr mean radiative heating rates over the Rub'al Khali Desert

Sea to construct the profiles of radiative cooling and warming rates, are relevant here. They noted a substantial warming over the dust layer which extended up to almost 600 mbs (4.5 km). Figures 45.7a and b from their study illustrate these respective profiles. Both the short-wave and the long-wave radiative heating/cooling rates are shown here. These 24-hour averaged profiles show a short-wave warming rate of

the order of 3°C/day over the top of the dust layer over Saudi Arabia, whereas over the adjacent Arabian Sea that warming is of the order of 2°C/day. The oceanic low clouds and the top of the massive dust layer exhibit a pronounced long-wave cooling rate of the order of 10°C/day. Overall, the dust aerosols appear to affect the short-wave warming rates and thus also the total heating rates over these dust-laden land and oceanic regions.

Mohalfi *et al.* (1998) have provided an estimate of the radiative effects of dust aerosols, based on the dust aerosol optical properties corresponding to the spectral wavelength 0.55 μm in Table 45.1, which is illustrated in Figure 45.8. The figure shows the difference between the dust-laden atmosphere and dust-free atmosphere for both short-wave (solid line) and long-wave (dashed line) heating rates. It can also be seen from the figure that Arabian dust is almost transparent to long-wave radiation. However, it indicates strong short-wave radiative heating up to 3°C/day at around 650 mb (4 km) which is just below the top of the dust layer. The diminished short-wave warming below 900 mb (1 km) reflects the reduction of solar incidence due to dust aerosols. Carlson and Benjamin (1980) and Sokolok and Golitsyn (1993) also noted similar types of radiative effects of dust layer over Saudi Arabia.

Mohalfi *et al.* (1998), furthermore, conducted several experiments with the Florida State University (FSU) limited area model to determine the sensitivity of dust aerosols on the synoptic features and diurnal variation of the heat low over the Arabian Peninsula. Their study revealed that the intensity of the heat low and its location is extremely sensitive to the radiative properties of dust aerosol. This is clearly depicted in Figure 45.9 which illustrates the variation of the

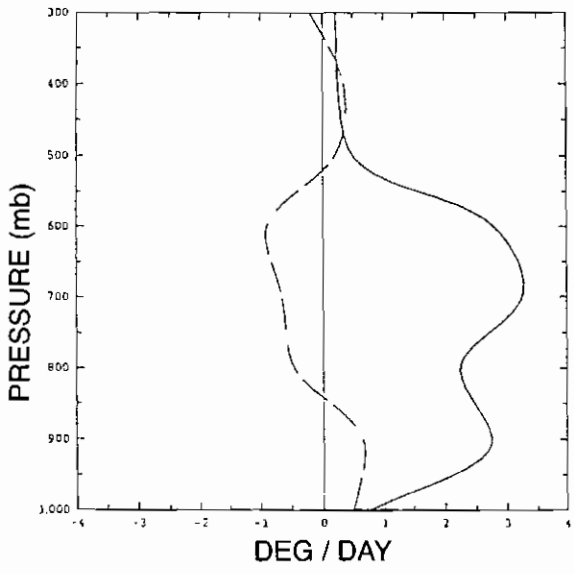

Figure 45.8 Difference in the short-wave and long-wave heating rates between dust-laden atmosphere from MONEX 1979 data, and those for the dust-free atmosphere calculated from the FSU model. These provide estimates of short-wave (solid line) and long-wave (dotted line) heating rates due to dust aerosols. Units: deg day^{-1}. (From Mohalfi *et al.* 1998)

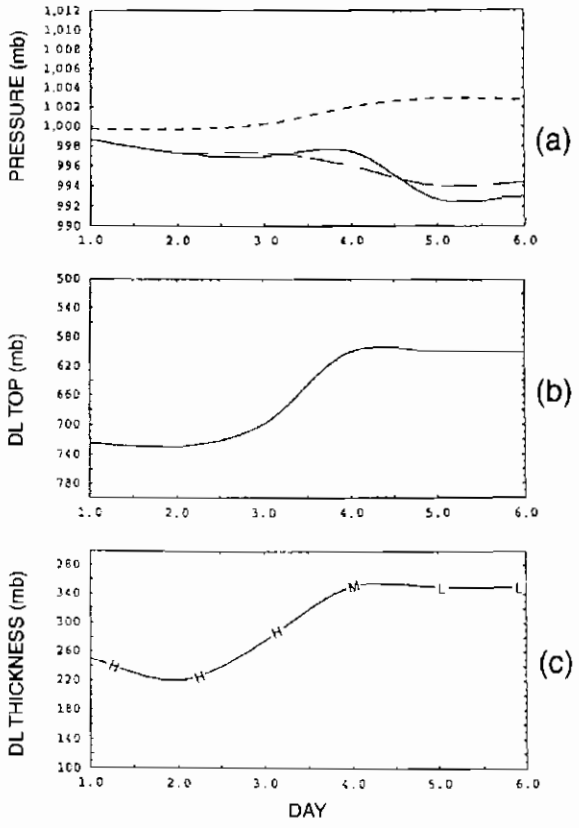

Figure 45.9 The intensity of heat low over the Rub'al Khali Desert (52°E, 21°N) in relation to height of the top and thickness of the dust layer. In the top panel, the solid line shows observed mean sea-level pressure of the heat low, dashed line, the mean sea-level pressure forecast by the aerosol experiment and dotted line shows the mean sea-level pressure forecast by the control experiment. (From Mohalfi *et al.* 1998)

mean sea-level pressure of the heat low with the height of the top of the dust layer and its thickness. The model which incorporates the dust aerosol in its radiative algorithm indicates an improved simulation over the control model. The cold advection from the northwestern Arabian Peninsula along with reduction of incident solar radiation inhibit the deepening of the heat low. However, radiative heating of the shallow dust layer below 700 mb (3 km) is sufficient to maintain the heat low as a low intensity trough. The heat low further deepens as the depth of the dust layer increases. This provides an increase in solar incidence in the presence of light dust aerosol resulting in more radiative heating of middle and lower levels, resulting in a fall of pressure. In addition, the study indicated that the dust aerosols not only absorbed and backscattered the solar radiation but also reduced the sensible heat flux at the lower levels which improved the simulation of the diurnal temperature variations in the region. An effect of the short-wave aerosol-related warming, especially over the middle troposphere over the Saudi Arabian Peninsula, is to enhance the easterly thermal wind over the open oceans to its south. The temperature anomaly associated with the dust layer in the lower troposphere over Saudi Arabia is cooler because of a reduction of direct solar radiation. This contributes to an enhanced westerly thermal wind, thus intensifying the Somali jet over the open ocean in the afternoon hours. Thus a diurnal maximum during the afternoon hours is modeled over the open ocean. This is the opposite of what we see over Somalia (Ardanuy 1979). Observations from the MONEX dropsonde observation during 1979 have confirmed such an out-of-phase relationship between the diurnal change of winds over the landmass of Somalia and over the open ocean of the north–central Arabian Sea.

HEAT AND MOISTURE SOURCES/SINKS OF THE MONSOON

The distribution of heat sources and sinks in the global tropics is found to be extremely important in simulating the tropical circulations (Gill and Philips 1986). Using a very simple linear shallow water model forced with locally isolated diabatic heating, Gill (1980) demonstrated that the major features of the monsoon can be simulated. Zhang and Krishnamurti (1996) extended this work further by studying the response of the analytical model using a more realistic global tropical heating distribution obtained from satellite-based datasets. Such a prescribed field is expanded into a low-order set of trigonometric functions in the east–west direction and parabolic cylinder functions (these are polynomial power functions used along the south–north direction to expand variables such as heating function, zonal and meridional wind and pressure) along the north–south coordinate. Figures 45.10a and b show the mean tropical circulations at 850 mb for July 1989 based on the European Centre for Medium-range Weather Forecasts (ECMWF) analysis and the corresponding analytical solution, respectively. From the figure, the following features in both the analysis and the analytical solution can be noted:

1 subtropical highs over the Pacific Ocean in both hemispheres;
2 subtropical highs over the Atlantic Ocean in both hemispheres;
3 Mascarene high over the southwestern Indian Ocean;
4 heat low over the Sahara;
5 heat low over Saudi Arabia;
6 heat low over the southwestern United States and Mexico;
7 monsoon trough over India;
8 trade wind system over the global tropics;
9 cross-equatorial flow over the western Arabian Sea; and
10 asymptotes of convergence defining the ITCZ over the global tropics.

A similar correspondence of the analytical solution with ECMWF analysis for January 1989 (winter circulations) was also noted. This emphasizes the importance of heat sources and sinks for the maintenance of tropical circulations.

Yanai *et al.*'s (1973) definition of apparent heat source (Q_1) and apparent moisture sink (Q_2) provides an invaluable tool for diagnostic studies of the monsoon. Here, we present Luo and Yanai's (1984) mean vertical distributions of heating and drying over a forty-day period (from May 26 to July 24, 1979) over four regions, namely western and eastern Tibet, the Yangtze River Valley over eastern China, and the

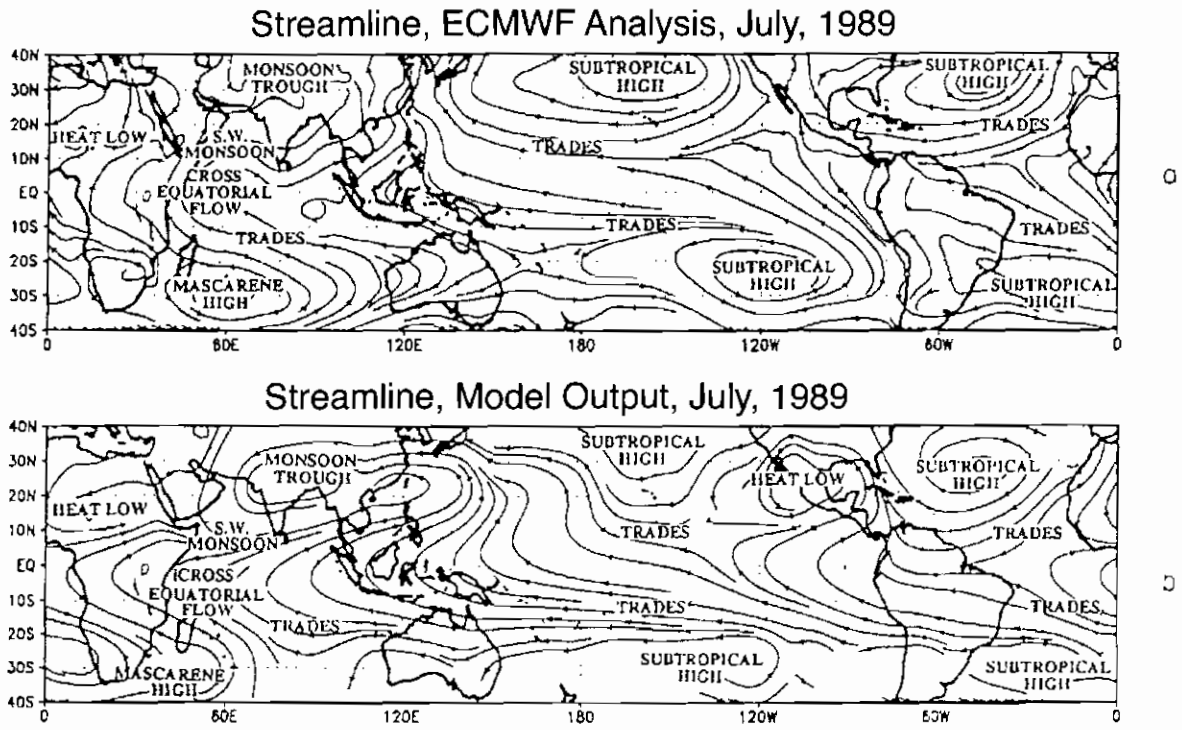

Figure 45.10 (a) Monthly mean of tropical circulation of July 1989, from ECMWF analysis. (b) Generalization of Gill's solution for the vertically integrated normalized heating distribution retrieved from OLR observations for July 1989. This solution describes nearly all of the major elements of the tropical summer climatology. (From Zhang and Krishnamurti.1996)

Assam Valley of northeastern India. These areas are characterized by relatively dry weather, moderate convective rain, steady stratiform rain and heavy convection, respectively. This is reflected in Figures 45.11a, b, c and d. Over the Tibetan Plateau, i.e. in regions I and II in Figure 45.11, and more so in the western Tibetan Plateau (region 1), it is characterized by large heating in the deep troposphere with very little moisture sink. Luo and Yanai (1984) point out that the forty-day mean profiles of Q_1 and Q_2 over region II represent the combined effects of two different conditions during this period: the pre-onset phase of the monsoon which is similar to the dry western plateau and the post-onset phase when convective activity begins. As a result, the profiles of Q_1 and Q_2 suggest weak moist convective heating in region II. Sensible heat flux calculated as a residual in the heat and energy budget equations revealed that it was a dominaut term in the equations, especially over region I. Furthermore, the diurnal variation of surface temperature is of the order of 12°C over most parts of the plateau. This strong surface heating offsets dry thermal convection which transports heat to the upper atmosphere. This is suggested by the existence of a deep well-mixed boundary layer with nearly constant potential temperatures over the western and central Tibetan Plateau. The mean vertical profiles of Q_1 and Q_2 over the Yangtze River Valley are very similar to each other, indicating that heating is mostly on account of frontal precipitation (primarily from stratiform cloud systems). Over this region, rainfall is primarily caused by the interaction between the summer monsoon winds from the south and airflow of mid-latitude origin from the north. The rainfall develops along a quasi-stationary front (called the Mei-yu Front) with most of the rainfall occurring on the warm side of the front. However, in region IV (over the Assam–Bengal region), the profiles of Q_1 and Q_2 have distinctly separated peaks which reflect the role of deep convection.

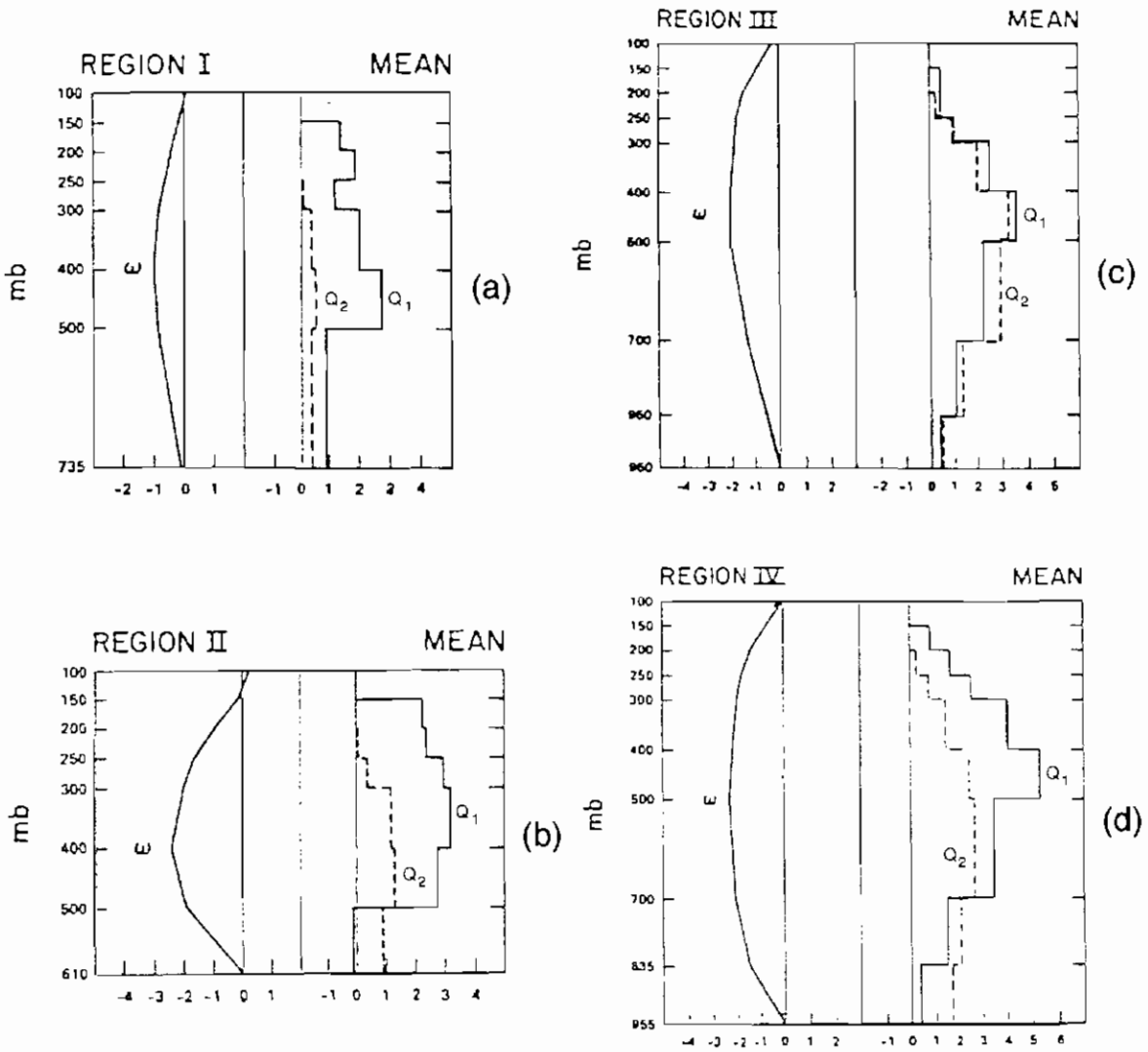

Figure 45.11 Forty-day mean vertical distribution of the areal mean vertical p-velocity (mb h^{-1}) and drying rate Q_1/C_p (K day^{-1}) over (a) western Tibet (region I), (b) eastern Tibet (region II), (c) Yangtze River Valley (region III), (d) Assam–Bengal region (region IV). These are based on Luo and Yanai (1984)

An important diurnal see-saw in local vertical circulation affects the weather of the northeastern foothills of the Himalayas and the Tibetan Plateau. Convection during the summer monsoon season is a maximum during the afternoon hours over the plateau, whereas it is a minimum in the early morning hours. The converse is true over northeastern India. This has serious implications in the understanding of the monsoonal heat source over these two regions. Figures 45.12a, b and c (from Kuo and Qian 1981) illustrate this see-saw very clearly. Further work is needed to clarify the distinct roles of these two regions.

When discussing any of the global monsoon systems, it is essential that one describes the primary large-scale drive of the monsoon, i.e. the differential heating. Krishnamurti *et al.* (1998a) have evaluated the basic components of monsoon energetics. In that study they allude to the importance of the covatiance of

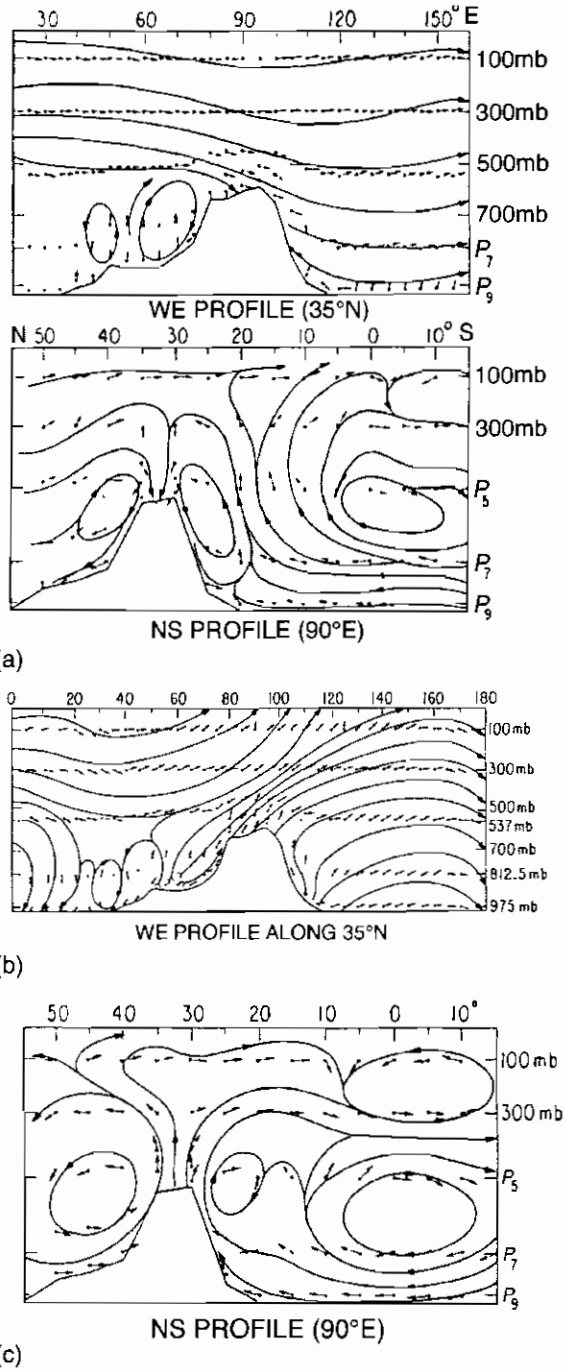

Figure 45.12 Simulated night-time mean vertical circulations. Top: (a) at 35°N W–E plane; bottom: at 90°E N–S plane with vertical velocity magnified 100 times. Simulated daytime mean vertical circulations: (b) at 35°N W–E plane; (c) at 90°E N–S plane. Vertical velocity magnified by 100

heating and temperature on the scale of the synoptic-scale monsoon as a measure of the differential heating. Furthermore, they show that the temperature field of a robust monsoon stays somewhat invariant in time in spite of this steady generation of eddy available potential energy. This happens because the divergent circulation simultaneously provides a robust covariance of the vertical velocity and the temperature, thus transferring the energy from the heat sources to the kinetic energy of divergent motions. These divergent motions do not exhibit any explosive increase in intensity. That happens because the divergent motions very effectively pass on the excess divergent kinetic energy to the rotational kinetic energy which is a key to the maintenance of the monsoon. The relative constancy in the strength of the monsoon, during an active spell, lies in the removal of the excess kinetic energy of the rotational motion via surface friction and via lateral transports out of the monsoon domain.

Another important feature related to the onset of monsoons is the depth of the moist layer of the monsoon, which extends from the surface to roughly 4 km over most regions. Prior to the onset of the monsoon the moist boundary layer is very shallow and extends up to only 1 km. As the onset occurs a deep layer of moist air (extending to almost 4 km depth) moves northwards from the Indian Ocean. This was noted by Joshi *et al.* (1990) using satellite datasets of total precipitable water and moisture retrieval techniques.

Li and Yanai (1996) have noted an important observational finding on the relationship between the onset of monsoon activity and the reversal of a meridional temperature gradient south of the Tibetan Plateau. Figure 45.13 shows the longitude–time section of the difference of the five-day layer mean temperature for 200–500 mb for the latitudes 30°N minus 5°N. This layer mean temperature gradient reverses (as shown by the shading) during the monsoon months, June through September, between 30°E and 150°E longitudes.

The monsoon energetics reviewed here are consistent with the description of the heating provided by Luo and Yanai (1984). The work of Luo and Yanai brings out the importance of heat sources ovet the eastern Tibetan Plateau and over the heavy-rain areas of northeast India. These are the regions where the

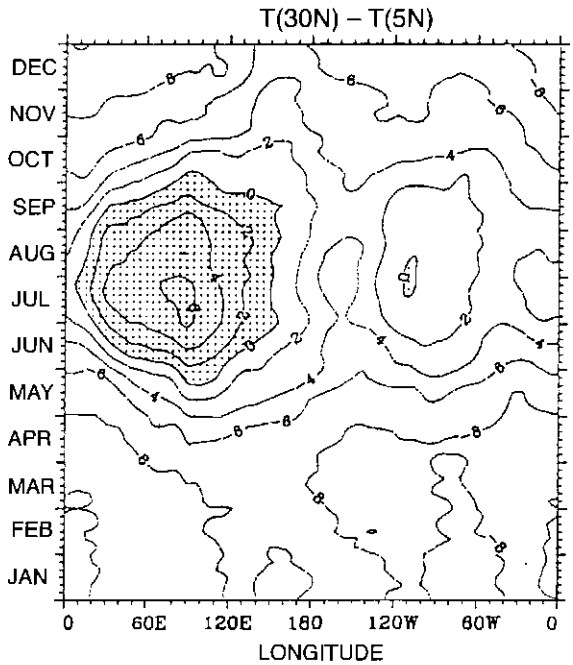

Figure 45.13 Longitude–time section of the difference of the five-day mean 200–560 hPa layer mean temperature (°C) between 5°N and 25°N. Regions of positive values (in °C) are shaded. (From Li and Yanai 1996)

contributions to the generation of eddy available potential energy are found to be the largest.

WINTER MONSOON

Winter monsoon rain affects the southeastern coasts of India and Malaysia, Borneo and northern Australia. Over most of these regions the lower tropospheric northeasterlies of the winter monsoon interact with the local orography to produce heavy rains. The rainfall over these regions is also attributed to the monsoon trough and monsoon disturbances. Furthermore, westward propagating tropical disturbances also contribute to the monsoon rains over these regions. The principal driver of the winter monsoon is a differential heating field that extends from the Siberian region (heat sink) to the maritime continent (heat sources). There also exists east–west-oriented differential heating between the equatorial eastern Pacific (heat sink) and the maritime continent (heat source). That picture is somewhat modified during El Niño (warm phase of the southern oscillation) years, when the east–west-oriented differential heating extends from the eastern to the central equatorial Pacific Ocean. The Walker circulation (this name refers to a vertical circulation along a west–east plane along the equator (and 5°S). This circulation has easterly winds near the Earth's surface, upward motion near Indonesia, westerly winds over the upper troposphere of the equatorial Pacific, and a descending lobe in the eastern Pacific Ocean is driven by the east–west-oriented differential heating.

The winter monsoon behavior cannot be entirely interpreted by these broad-scale heating differentials. There exist a plethora of smaller space–time scale transients within the winter monsoon environment that are driven both by local heat sources and sinks and by local dynamical instabilities. (The presence of horizontal and vertical wind variation, called shear, can lead to dynamical instabilities where smaller scales can grow at the expense of energy they receive from the larger-scale shearing flows.) It is from the detailed prediction of such transients that one often learns of the importance of these more regional dynamical and thermodynamical forcings. One of the important features of the winter monsoon is the ITCZ which is located some 10° latitude south of the equator. The cloud cover along this east–west-oriented axis of rainfall shows a considerable degree of intermittency. Figures 45.14a, b, c and d illustrate the rainfall variability, during different months, based on Krishnamurti *et al.* (1997c). This covers a four-month period during December 1992 through March 1993. The rainfall estimates were derived from a microwave instrument, the Special Sensor Microwave Imager (SSM/I), on board a polar orbiting satellite. This rainfall variability has spectral peaks on the time scales of 4 to 6 days and the Madden Julian time scale of 30–50 days. (This refers to a 40–60-day time scale that was first brought to the attention by Madden and Julian 1971; these are eastward propagating planetary waves that traverse the globe in that period. The largest amplitude of this oscillation is near the equator.) The 4–6-day variability arises from considerable storm activity on the summer hemisphere side of the ITCZ where an abundance of westward propagating tropical waves and tropical cyclones are usually present.

The shallow vertical structure of the winter

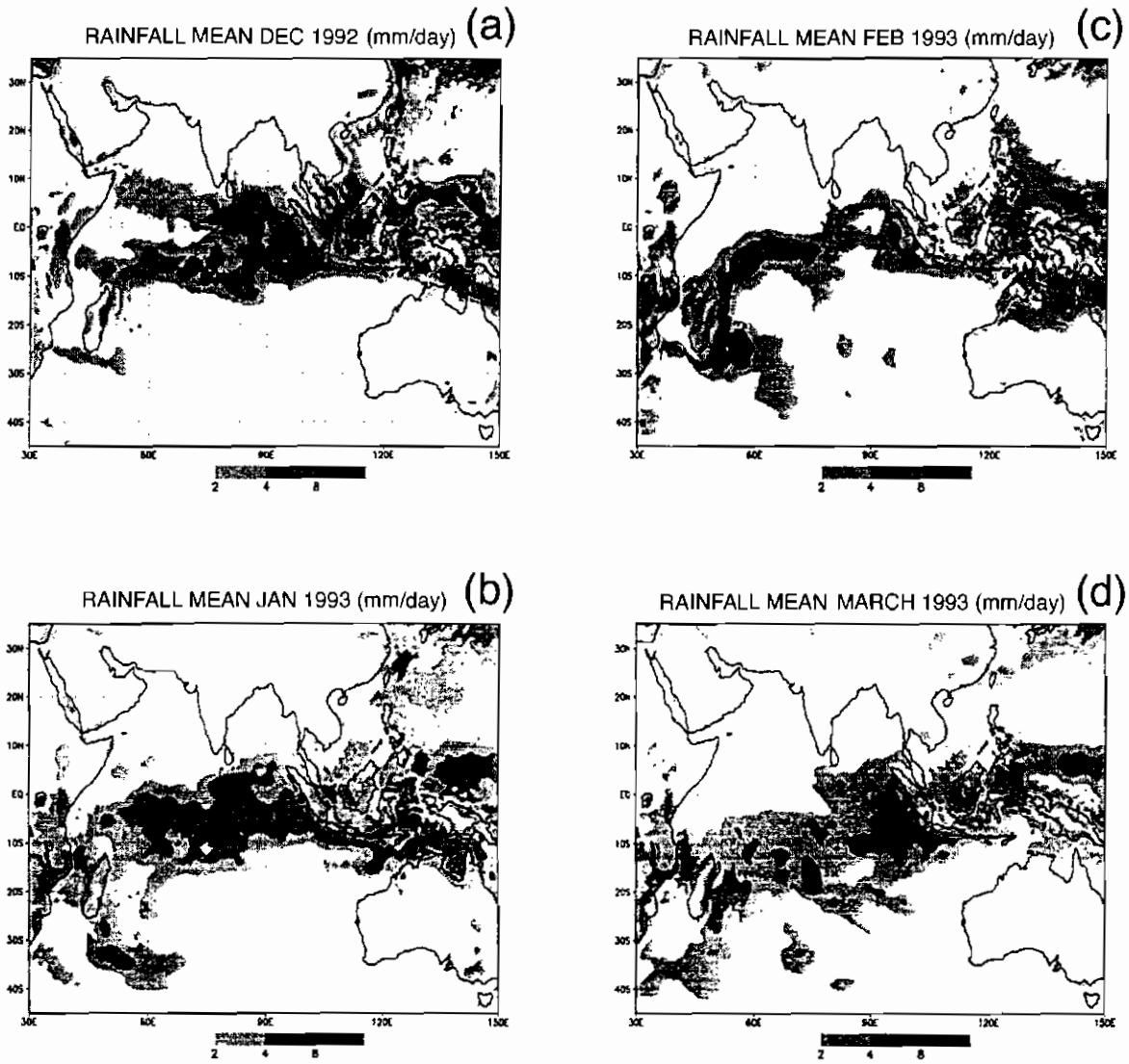

Figure 45.14 Monthly mean daily rainfall ending 12 UTC. For (a) December 1992, (b) January 1993, (c) February 1993, (d) March 1993. Units: mm/day; the rainfall amounts over shaded areas are according to the scale shown below each figure

monsoon, especially north of 15°N, distinguishes it from the summer monsoon. The winter monsoon winds which are northeasterlies near the Earth's surface turn towards westerlies over a very short vertical distance. Near 20°N this depth of the winter monsoon northeasterlies is about 1.5 km. This depth increases slowly as one proceeds south towards the ITCZ. At 10°N this depth is around 3 km. Pollutants are transferred equatorwards by these shallow northeast monsoon circulations. These pollutants are possibly carried upwards as they enter the convective regions of the ITCZ. This is a topic of major interest for the cloud chemistry and cloud radiative interaction program for the proposed Indian Ocean Experiment (INDOEX) which is planned for 1999. These winter monsoon circulations over the Arabian Sea are mostly from the north below the 1 km level; they turn to easterlies in the next kilometer, and very rapidly

become westerlies above that level.

Regional scenarios of the winter monsoon include phenomena such as the cold surges from the Asian mainland traversing down the South China Sea. These have been very well documented by Lau and Chang (1987). They show a southward propagation of discontinuities in temperature (of a couple of degrees), meridional wind and especially the humidity. The phase speed of propagation is that of Rossby gravity waves (these describe the typical wave motions in the tropical latitudes, are solutions of the meteorological equations and describe the speed of propagation of systems such as the tropical easterly waves; the typical propagation speed of these waves is around 7° longitude/day). As this surge arrives over the middle of the South China Sea, the discontinuities tend to weaken considerably. Westward propagating ITCZ or equatorial waves from the western Pacific Ocean often interact with these surges resulting in the formation of surge vortices. These vortices often become intense rain-producing small tropical depressions causing heavy rains over east Malaysia. The cold surges also tend to amplify the ITCZ over the Java Sea, bringing in moisture from the South China Sea. There have also been instances when this evaporation is small and the cold surges arrive as dry surges, resulting in a weakening of the ITCZ over the maritime continent and resulting in an eastward shift of the ITCZ activity to the western Pacific Ocean. This entire region has large divergent wind fluctuations on the time scale of the Madden–Julian Oscillation on synoptic and larger spatial scales. These systems have been studied in the context of the onset of the Australian monsoon and its active and dry spells (see Krishnamurti *et al.* 1995a; Davidson 1995).

NUMERICAL WEATHER PREDICTION

In this section we summarize the recent emphasis on the numerical weather prediction of the monsoon. This review outlines the following areas: impact of model resolutions, organization of resolved convection and the sensitivity to cumulus parameterization.

Most operational weather centers that deploy global models have examined the performance of their models with reference to monsoon forecasts (see Mohanty *et al.* 1994). The centers in India, Australia, NCEP (USA), ECMWF (England), the UK Meteorological Office and Japan have routinely examined the performance of their models. Based on their evaluations, we note that the predictability over a monsoon domain, measured from the 500 mb (5.8 km) geopotential height anomaly correlations greater than 0.6, is generally of the order of two to three days. (Geopotential height anomaly correlations refer to a forecast skill parameter. Here one first removes the climatology of the predicted and the observed fields. The correlation of the departure, from climatology, fields are called anomaly correlations.) The limitations stem from various factors such as the treatment of deep convection, steep orography and the overall coverage and quality of observations. As a result, progress has been quite slow. Research models have addressed various issues related to the monsoon forecasts, some of which are summarized below. The impact of resolution is best illustrated by Figure 45.15. Here, we show the day 5 predicted position of the center of a monsoon depression (shown by black dots) for various resolutions of a global model. These resolutions range from T21, T31, T42, T63, T106 and T170. The analysis, based on ECMWF, for this verification period (i.e. corresponding to day 5 of the above forecasts) is superimposed. This shows the "observed" flow fields at 850 mb. This is a typical forecast that illustrates that the improvements in medium-range forecast result from increased resolution. The better forecasts arose at the resolutions T106 and T170. These results also reflect the improved representation of orography at such higher resolutions. The resolution issue has also been very revealing in another major area of monsoon prediction. That relates to predicting the organization of meso-convective precipitation in the maintenance of and in the medium-range prediction of the monsoon. Physical initialization, described in Krishnamurti *et al.* (1991), is important for this study. Here, the observed rain rates were obtained from a mix of satellite (SSM/I- and OLR-based algorithms) and rain-gauge data following Gairola and Krishnamurti (1992). Using reverse cumulus parameterization and reverse similarity algorithms, these rain rates were assimilated within a very high resolution global model. The resolution of the global model, T255, is the highest of any current operational model (globally). The transform grid separation at resolution T255 is comparable to the

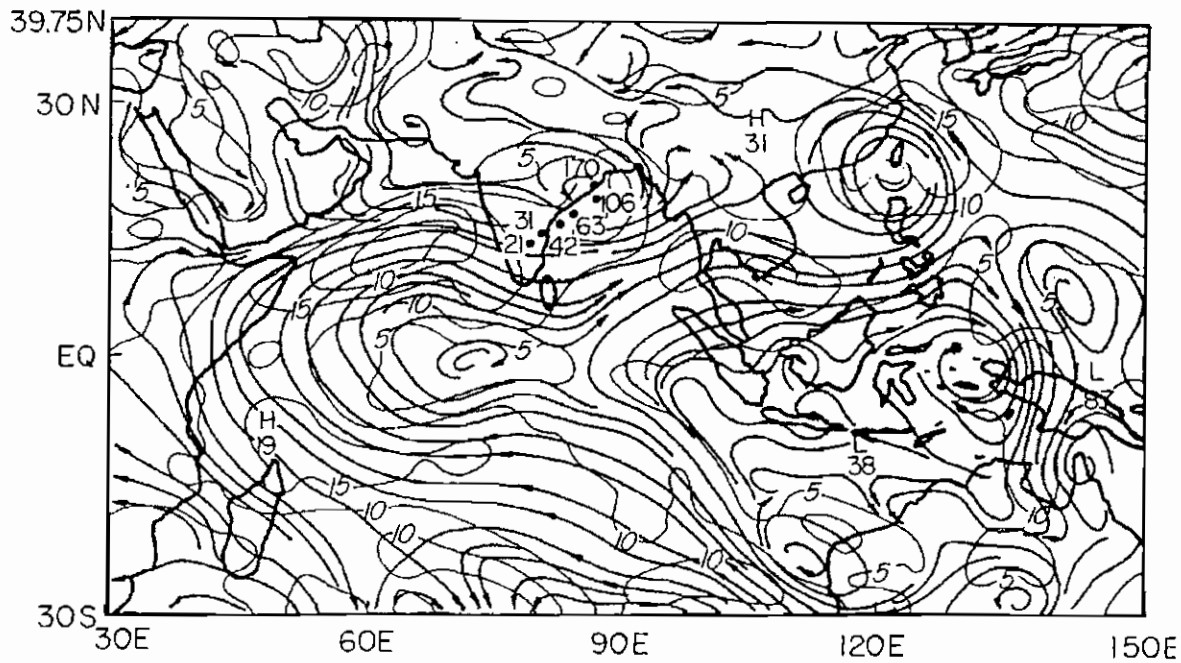

Figure 45.15 Day 5 predicted positions of the monsoon depression (shown by black dots) for resolutions T21, T31, T42, T63, T106 and T170

footprint of the SSM/I instrument, i.e. roughly 35 km^2 at 20°N. This makes it possible to initialize the observed rainfall without undue smoothing. Figures 45.16a and b illustrate such a rainfall obtained from observations and from the model's initialization. These fields have a correlation of 0.92. When global forecasts are made at this resolution the meso-convective distribution of monsoon rainfall is preserved in general over several days. One of the major outcomes of these numerical weather prediction experiments is that convection is organized on the scales of the synoptic-scale monsoon and as a result two things are notable:

1 The two-dimensional spectra of the covariances of the vertical velocity and temperature and of the convective heating and temperature show a maximum variance on the scale of the monsoon.
2 The anomaly correlation, a measure of skill score of forecast error, are higher for these high resolution forecasts compared to un-initialized lower resolution forecasts of the monsoon.

Figure 45.17 illustrates the two-dimensional spectra of the vertical velocity and temperature ($\overline{-\omega' T'/P}$) for the above model at the resolution T255 and for an NCEP reanalysis at T62 without any physical initialization. The lower resolution exhibits a maximum variance for the zonal scale, which indicates an overemphasis of the local Hadley overturning. The higher resolution places the energy conversions on the synoptic scales of the monsoon. The message that emerges here is that the organization of convection is better conveyed by a higher resolution model with physical initialization. The observed and predicted meso-convective precipitation elements at hour 72 of forecast are shown in Figures 45.18a and b, where we see a considerable model skill in predicting the organization of convection. The anomaly correlation of the 500 mb stream function over a monsoon domain 30°E to 150°E, 30°S to 40°N for three different models are shown in Figure 45.19. (Anomaly correlation denotes a flow field parameter such that the flow is along lines of constant stream function. Here one removes the divergent wind before constructing the isopleths of the stream function. This flow is non-divergent.) Here, we are comparing the results from T62 and T106 resolutions without physical initial-

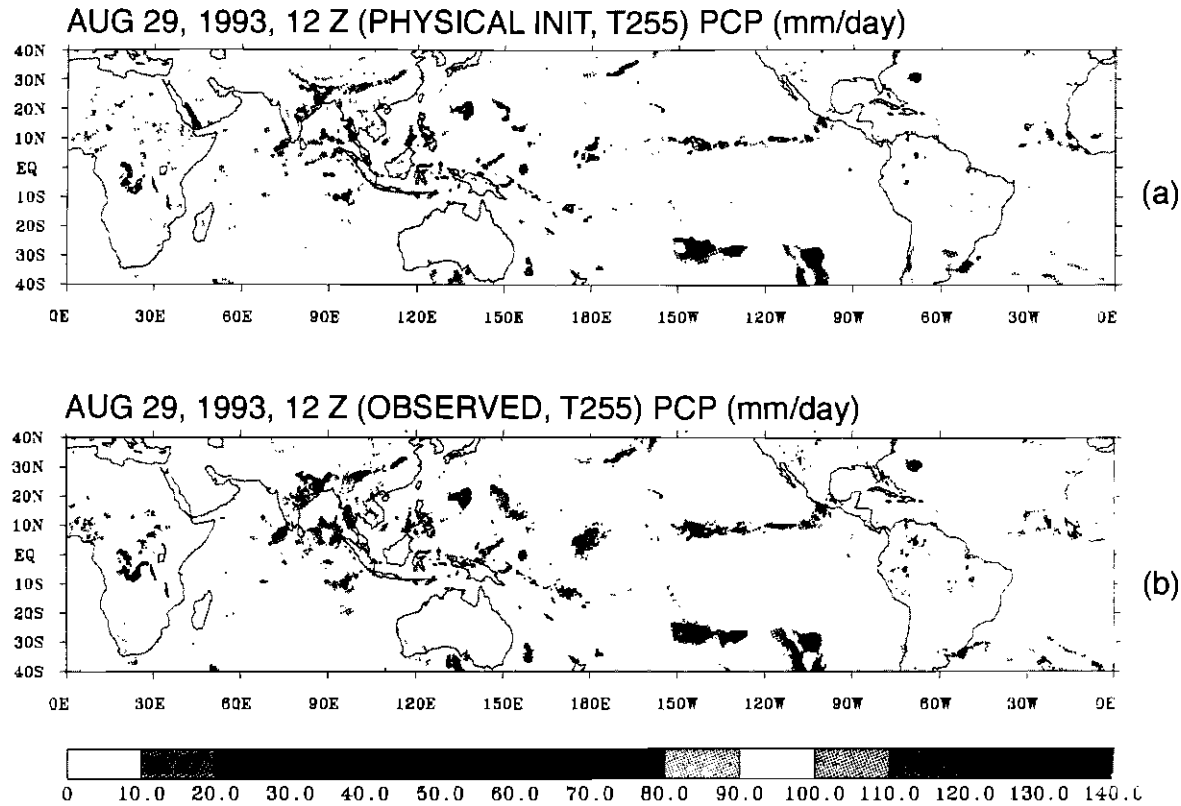

Figure 45.16 A comparison of physically initialized and observed rainfall at 12 UTC of August 29, 1993; units: mm/day. (From Krishnamurti *et al.* 1998b)

ization (this refers to a data assimilation procedure for a numerical weather prediction model where the data analysis incorporates the initial observed rain rates within the analysis) and for the above T255 resolution with physical initialization. These results suggest the possible importance of physical initialization at very high resolution for monsoon forecasts.

Finally, we shall briefly address the issue of the onset of monsoons. The UK Meteorological Office has made some important strides in the prediction of the onset of Indian monsoon rainfall. One of the major issues in the prediction of monsoon is its sensitivity to the parameterization of cumulus convection. This is especially true for the onset forecasts as well. It is easy to demonstrate that a classical Kuo-type scheme (an early scheme developed by Kuo 1965, when the effects of cumulus convection, i.e. the heating, moistening and rainfall rates are incorporated in a numerical weather prediction model using the properties of a local moist adiabat) that underestimates convective heating performs very poorly in resolving the onset as compared to a more robust modified Kuo-type scheme (advancement of the early scheme of Kuo 1965, where the heating, moistening and rainfall rates for a numerical weather prediction model are statistically corrected using field experiment datasets; Krishnamurti and Bedi 1988). Figures 45.20a, b, c and d illustrate this sensitivity. In these illustrations we show an initial state at 850 mb for hour 0, i.e. June 11, 1979, 12 UTC, the hout 144 predicted fields for the two different cumulus parameterization schemes and the corresponding observations. The more robust scheme illustrates the formation of an onset vortex over the northern Arabian Sea and the onset of strong westerlies from the Arabian Sea towards southern India. These were not predicted from the simpler

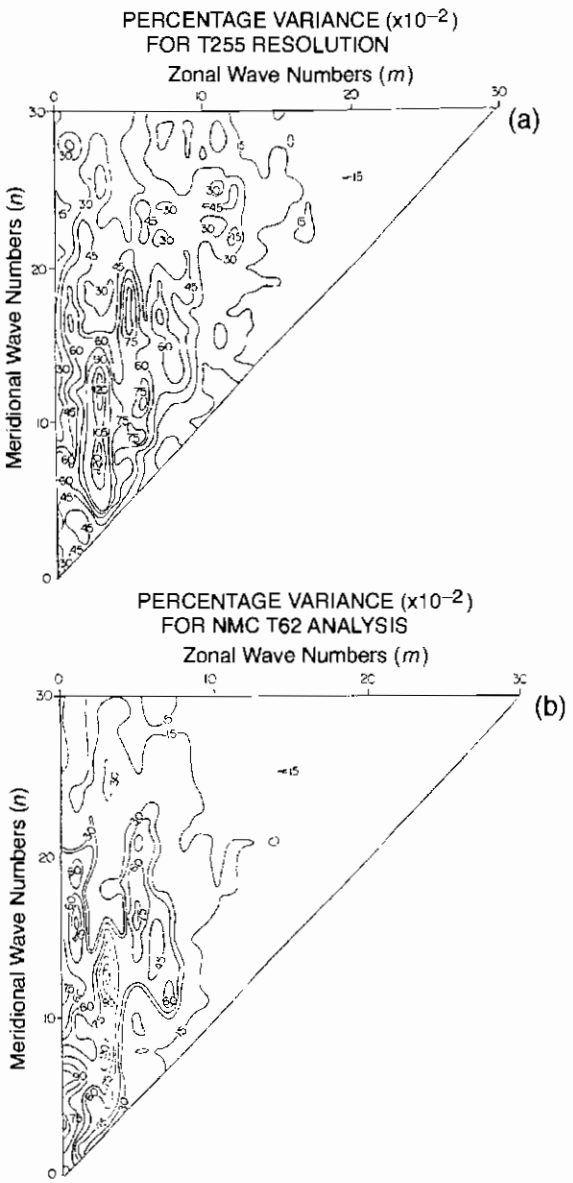

Figure 45.17 Distribution of vertically integrated percentage variance of $-(\overline{\omega' T'}/p)$ in two-dimensional wave number (m, n) domain (triangular truncation space): (a) for T255 resolution run; (b) for T62 reanalysis data. (From Krishnamurti et *al.* 1998b)

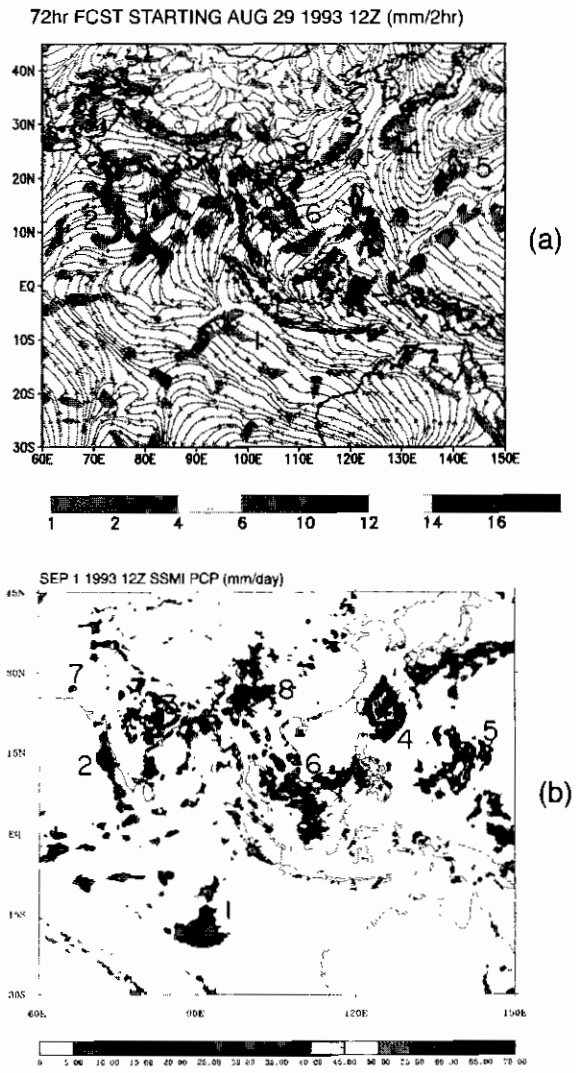

Figure 45.18 The observed and predicted meso-convective precipitation at hour 72 of forecast at T255 resolution

version of the cumulus scheme which retained an essential anti-cyclonic flow over the Arabian Sea for the entire six-day period. Resolution, orography and the handling of cumulus convection are important ingredients for improvements of monsoon forecasts.

INTRASEASONAL VARIABILITY

The Asian summer monsoon exhibits significant variance in the 30–50-day time scale. Many observational studies in the monsoon region have shown the meridional propagation of clouds (Yasunari 1981; Sikka and Gadgil 1980), precipitation anomalies (Singh and Kripalani 1985, 1986), and of the trough and ridge lines that are associated with the wet and dry spells of

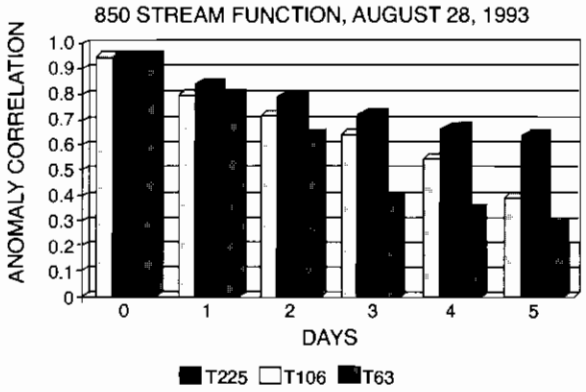

Figure 45.19 Anomaly correlation of 500 mb stream-function forecasts at resolutions T255, T106 and T63 (From Krishnamurti *et al.* 1998b)

the Asian summer monsoon (Krishnamurti and Subramaniam 1982) on this time scale. Hartman and Michelsen (1989) examined seventy years of Indian monsoon rainfall data and noted clearly dominant oscillation on the time scale of 30–50 days. This was most pronounced south of 23°N and clearly exhibited a northward motion from the equatorial latitudes of the Indian Ocean. The scale of these systems is roughly 2,000–3,000 km with an approximate speed of 1° latitude/day. Figures 45.21a and b (based on Krishnamurti *et al.* 1992a), illustrates a latitude–time diagram of the outgoing long-wave radiation (OLR) and the precipitation averaged across 70°E to 85°E. It is evident from the figure that the origin of these meridionally propagating systems is near the southern

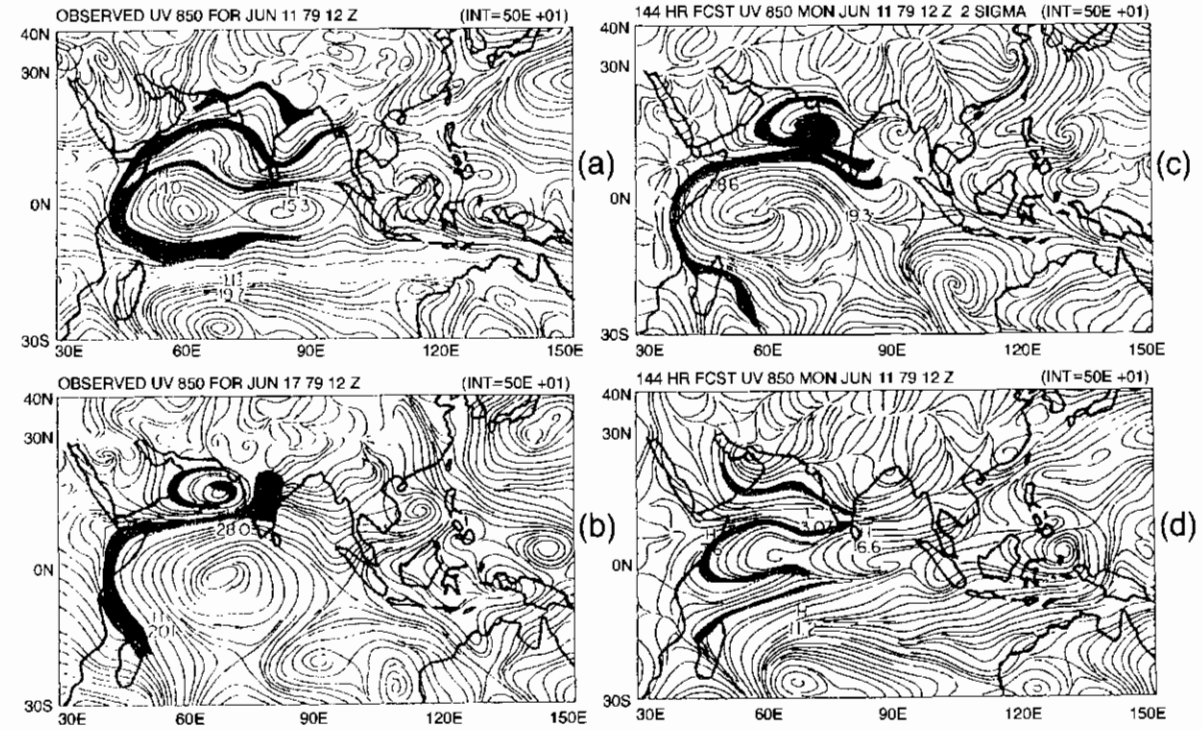

Figure 45.20 An 850 mb flow field showing the stream lines and isotachs (m s^{-1}). (a) Obtained from ECMWF analysis for the start date of the forecast, i.e. June 11, 12Z, 1979. (b) Obtained from ECMWF analysis for June 17, 12Z, 1979, (c) After a 144-hour forecast valid for June 17, 12Z, 1979, with the modified Kuo (Krishnamurti and Bedi 1988) convection scheme. (d) After a 144-hour forecast with Kuo (1965) convection scheme. (This is based on Krishnamurti and Bedi 1988)

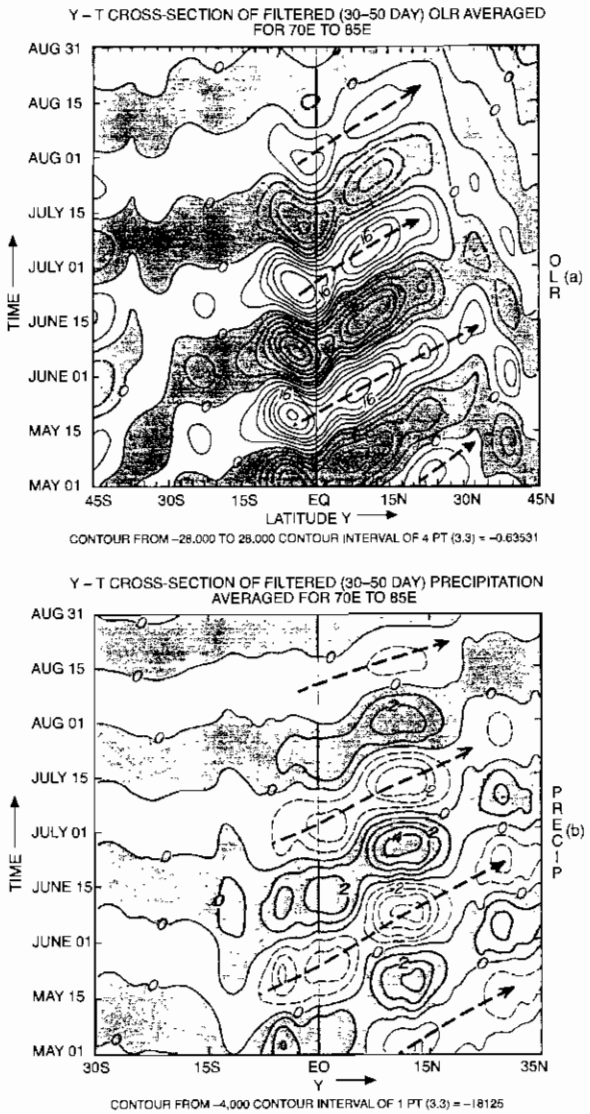

Figure 45.21 Latitude–time diagram showing meridional propagation in time. The values are averaged zonally from 50°E to 70°E. Panel (a) shows the outgoing long-wave radiation on the time scale of 30–50 days. Panel (b) shows the rainfall derived from an OLR algorithm, again on the same time scale

equatorial trough, i.e. near around 5°S. In Figures 45.22a and b, we present histograms that illustrate the percentage variance for the zonal harmonics (here, one performs Fourier analysis along latitude circles in order to determine the phase, amplitude and variances of different waves of which a zonal dataset is composed) of the 850 mb flow on the time scale of 30–50 days at different latitude belts over the Northern and Southern Hemispheres, respectively. Similarly, Figures 45.22c and d show the percentage variance for the zonal harmonics at 200 mb. It is apparent from the figure that most of the variance is explained by the first six or seven harmonics with higher latitudes exhibiting larger spread through wave number seven or eight. While exploring the global variability of the intraseasonal oscillation, Krishnamurti *et al.* (1992a) noted a strong correlation in the variability of the zonal flow of the monsoon, atmospheric angular momentum and length of day. The active periods of the monsoon are accompanied by east–west flow accelerations which increase the atmospheric angular momentum, thereby increasing the length of the day in order to maintain the invariability of the total angular momentum. Likewise, during the break periods of the monsoon a decrease in the length of the day was noted.

Lau and Chan (1985) have observed intraseasonal oscillations in the near equatorial organized super-cloud clusters which move eastward at a speed of roughly 10° longitude/day. Embedded within these clusters, Nakazawa (1988) noted smaller cloud systems that moved westwards at a speed of roughly 5° longitude/day. Such westward propagating systems have also been noted in the wind analysis by Murakami (1984). The super-cloud cluster is an envelope whose eastward motion is on the time scale of 30–50 days.

The intraseasonal variability in the monsoon has also been found to modulate the tracks of the typhoons. In a recent study, Chen and Weng (1996), analyzed the tracks of the summer typhoons in the western north Pacific between 1979 and 1993. Here they noted intraseasonal variations between straight and recurving tracks. They associated the meridional propagation of the typhoons to the low-level 30–60-day oscillation of the monsoonal trough–ridge systems. They determined that the typhoon track recurves if the northward translation can move the typhoon to the mid-latitude westerlies which are associated with deepening upper-level short-wave troughs over East Asia. However, the typhoon track would be straight moving if the northward translating typhoon fails to reach the westerlies due to the blocking phenomenon of the Tibetan or subtropical Pacific high.

Wang and Xie (1997) proposed a model for this

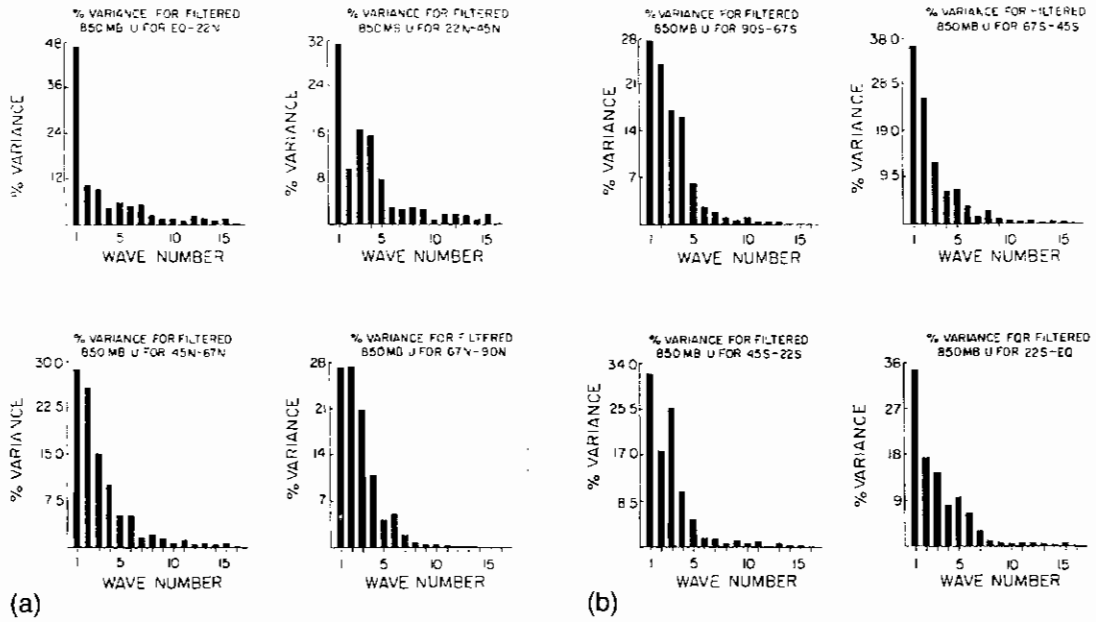

Figure 45.22 (a, b) Histogram illustrating the percentage variance for the zonal harmonics of the 850 mb flow on the time scale of 30–50 days. These panels include the results for eight latitude belts: equator to 22°N, 22°N to 45°N, 45°N to 67°N, 67°N to 90°N; 90°S to 67°S, 67°S to 45°S, 45°S to 22°S, and 22°S to equator. (From Krishnamurti *et al.* 1992)

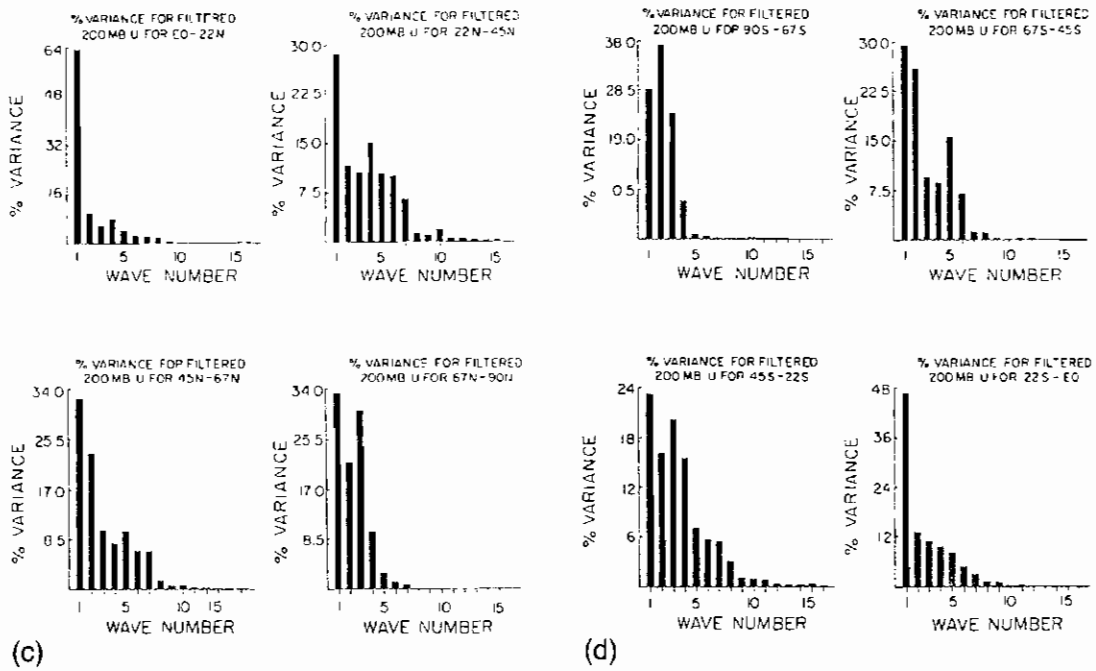

Figure 45.22 (c, d) Histograms illustrating the percentage variance for the zonal harmonics of the 200 mb flow on the time scale of 30–50 days. These panels include the results for eight latitude belts: equator to 22°N, 22°N to 45°N, 45°N to 67°N, 67°N to 90°N; 90°S to 67°S, 67°S to 45°S, 45°S to 22°S, and 22°S to equator. (From Krishnamurti *et al.* 1992)

transient behavior of eastward and meridional propagation of the intraseasonal oscillations in the Northern Hemisphere summer. Here, a coupled Kelvin–Rossby wave packet (this alludes to a near equatorial wave that traverses eastward, and associated with upwelling and colder waters above which the atmosphere was relatively dry) was first noted as a disturbance over the east coast of Africa which moves eastward. On account of reduced moisture availability and mean sinking motion over the central eastern Paeifie, convection is generally suppressed. This results in the decay of the equatorial Kelvin–Rossby wave packet. The convectively active region in the western Pacific with a mean upward motion and high moist static energy (total energy per unit mass of air measured by $gz + C_pT + Lq$ where gz denotes potential energy, C_pT denotes sensible heat and Lq denotes the latent heat) provide a favorable environment for the emanation of moist Rossby waves. These waves move northwestward toward Southeast Asian monsoons. As a result of the prevalent asymmetric distribution of monsoons, easterly vertical shear and the seasonally enhanced moist static energy, the Rossby waves amplify and develop into asymmetric structures with respect to the equator. These Rossby waves, on their approach towards the sinking dry air mass over the Middle East and North Africa, start to stall and decay. However, the asymmetric structure of the Rossby wave combined with the mean Hadley eirculation of the summer monsoon, reinitiates an equatorial convective disturbance that propagates eastward, which marks the beginning of the next cyele of the low frequency disturbances.

Furthermore, Krishnamurti *et al.* (1992a), whilc examining the vertieal variations of these oscillations, noted that they exhibited distinet dynamical structures in the tropics and the mid-latitudes. Figures 45.23a and b represent the vertical phase of these oscillations in the zonal flow for the tropics, while Figures 45.23c and d represent the mid-latitudes. Phase reversal between the lower and upper troposphere in the tropical convective ateas is evident in Figures 45.23a and b. A barotropic structure (an atmosphere where the pressure and density surfaces coincide, and as a consequence pressure and temperature isopleths do not interseet and there is no vertical variation of the horizontal wind) in the mid-latitudes is discernible in Figures 45.23c and d. These structures indicate the

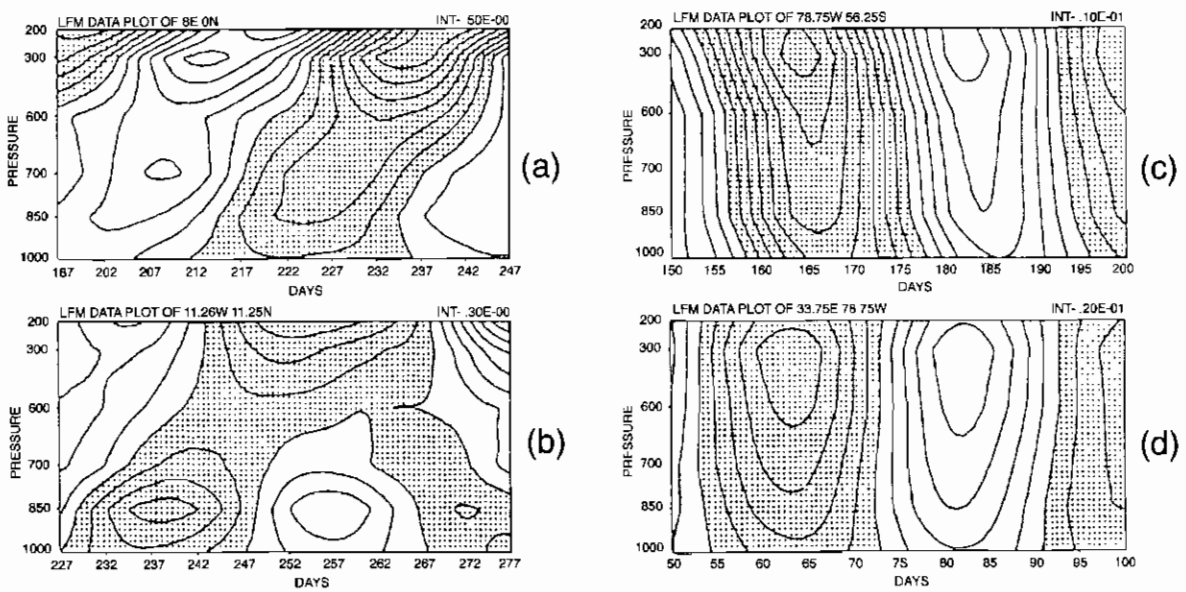

Figure 45.23 Pressure–time analysis of the zonal wind on the time scale of 30–50 days for two tropical grid prints (a) and (b) and for two higher latitude grid points (c) and (d). The units are in m s^{-1}. Shaded areas denote negative values. The interval of analysis is shown at the top right of each panel. (From Krishnamurti *et al.* 1992a)

importance of convection in the tropics and of dynamics in the higher latitudes for the generation and maintenance of these oscillations.

Tropical mid-latitude interaction on intraseasonal time scales

Several studies (e.g. Palmer 1988; Weickmann *et al.* 1985) have found significant tropical and extratropical interaction on the intraseasonal time scale. One of the common observations that has often been made is that the amplitude of the extratropical response to convective anomalies is larger during those periods when OLR anomalies propagate eastward from the Indian Ocean to the central Pacific. Using First GARP Global Experiment (FGGE) Level III-b wind and temperature analyzes at 200 mb and OLR datasets from TIROS-N satellite, Magana and Yanai (1992) showed that the intraseasonal modulation of the convective activity and its extension from Indian Ocean to the Central Pacific and over Central America regulated the amplitudes of the South Asian high and mid-Pacific trough through upper-level divergence over Southeast Asia and convergence over the central North Pacific. In addition, the transients around the subtropical circulation provide robust mechanisms for the tropical–mid-latitude interactions on the 30–50-day time scales. Figure 45.24, based on Magana and Yanai (1992), illustrates the variability of the relative angular momentum (this measures the angular momentum of a parcel of air relative to the Earth as it is measured by $f[r^2/2]$ where f is the coriolis parameter and r is the distance of the parcel of air from the center of the Earth) at 200 mb in the Northern Hemisphere through time series of anomalies of zonally averaged east–west wind ($[u]'$) at every 5° latitude interval. The variations in the field are closely associated with the intraseasonal oscillation which is superposed over it. This signal propagates meridionally from 10°N to 40°N modulating the mid-Pacific trough.

Krishnamurti *et al.* (1997b) viewed the wave energy flux across the critical latitude separating the tropical easterlies from the extratropical westerlies using a complete non-linear system for the north–south wave energy flux in the frequency domain. This included linear, and quadratic and triple product non-linearities which were handled using Hayashi's (1980) co-spectral

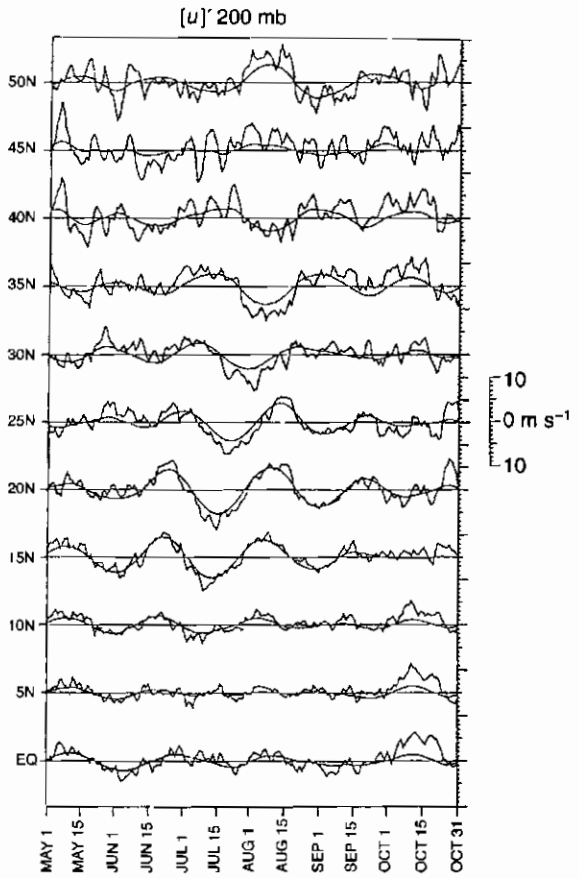

Figure 45.24 Time series of anomalies of zonally averaged zonal wind at 200 mb during the NH summer (thick lines) and their band-pass (30–60 days) filtered versions (thin lines). (Based on Magana and Yanai 1992)

method (spectral analysis to determine the lag relationship phase as well as amplitude between time series of two variables in wave number domain). Such a non-linear formulation of the wave energy flux showed a distinct continuity of the fluxes from the latitudes of the monsoon all the way to the polar latitudes. This is illusttated in Figures 45.25a, b, c, d, e, f, g and h for the eight years from 1987 through 1994. Here, the ordinate denotes the latitude and the abscissa denotes time. A strong convergence of wave energy flux in the polar latitudes provides a possible explanation of the observed polar maxima of the zonal flow amplitudes on the 30–50-day time scale in the upper ttoposphere and the lower stratosphere.

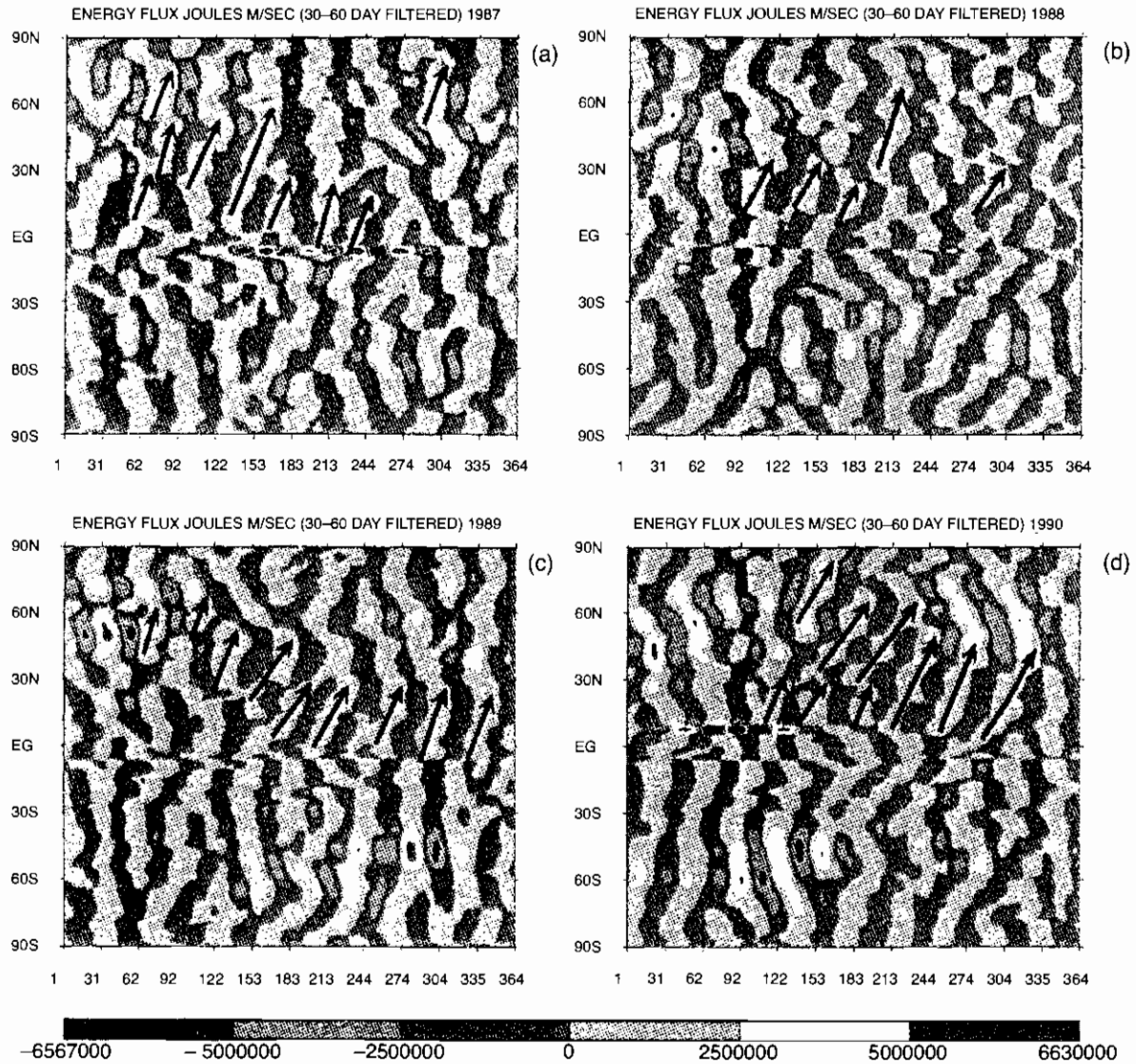

Figure 45.25 (above and opposite) Latitude–time diagram of meridional wave energy flux $\overline{\phi' v'}$ on the time scale of 30–50 days. Eight separate years of results are shown for the years 1987 through 1994. The ordinate denotes latitude, the abscissa denotes day of the year. Units are Joules m/sec. The heavy arrows denote channels of strong meridional poleward flows. (From Krishnamurti *et al.* 1997b)

However, the linear theories, which assume a constancy in time for the zonal flows, preclude any direct interaction across the critical latitude. It only accounts for episodic opening of the barrier during periods of extension of zonal flows beyond the mean critical latitude initiated by the pulsating mid-Pacific trough (Lu and Yanai 1987; Webster and Zhang 1989). Since the zonal flow anomalies on the time scale of 30–50 days propagates meridionally, in effect the critical latitude itself propagates. It is this migration of the transient critical latitude that permits a meridional leakage of wave energy flux across a critical latitude defined from a time mean flow.

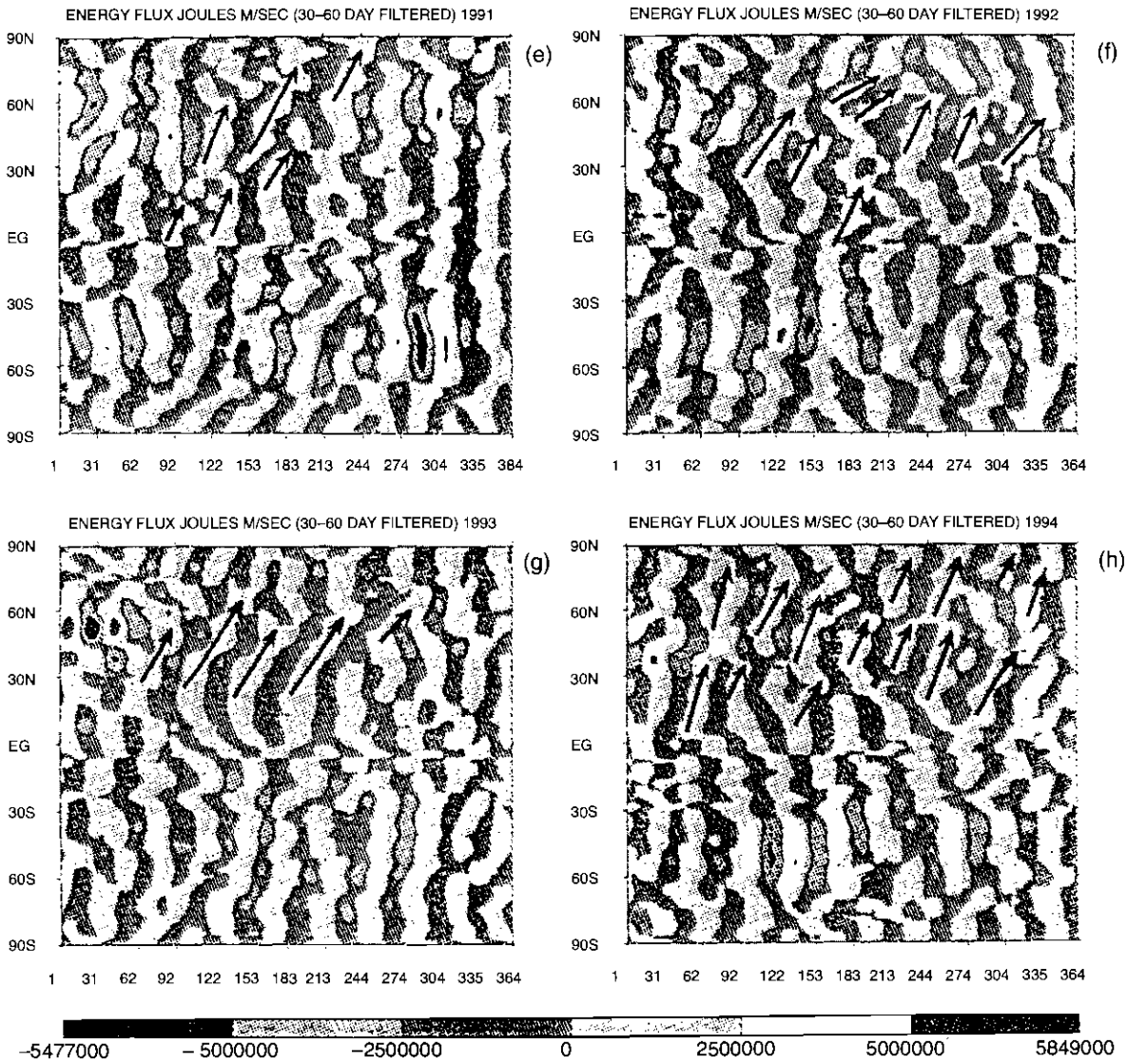

Predictability of low frequency models

Krishnamurti *et al.* (1990a, 1990b, 1993) have demonstrated that the intraseasonal variability associated with the monsoons over India, China and Australia can be predicted through one cycle, i.e. thirty days. The methodology adopted for such a forecast involves a primitive equation-based comprehensive global spectral model (this refers to a global forecast model where spherical harmonics are used as basis functions and these equations are cast in terms of spectral coefficients of these harmonics, see an advanced text on numerical weather prediction for details) with full physics (this refers to a model that includes convective, radiative and planetary boundary layer processes) and a unique initial state. Anomalies derived on the 30–50-day time scale using a bandpass filter are superposed on the seasonal mean, which determines the initial state for such extended forecasts. This is based on the premise that the contamination of the low frequency modes can be

delayed by suppressing the high frequency motion of the initial state. A typical forecast skill from such an experiment is shown in Figures 45.26a and b for the global and tropical domains. Here, the skill is measured in terms of anomaly correlations of the low frequency 850 mb wind component. Invariably, the skill beyond five days of the forecast drops from 0.5 to 0.2. From the figure it is seen that the anomaly correlations are maintained at around 0.5 even after day 30 of the forecast with the adopted initialization procedure; however, a sharp drop of skill in the first five days is noted. The authors reason that, although the initialization procedure filters out the high frequency motions in the initial state, it has no control over its tendencies, which might initially contaminate the low frequency motions as these higher frequencies evolve. This skill of large-scale circulation fields is then used to provide an outlook forecast on dry and wet spells of the monsoon. A schematic illustration of such a forecast is shown in Figures 45.27a, b, c, d, e and f. When the climatological circulation is in phase with the low frequency circulation in the lower troposphere (as in Figures 45.27a, b and c) a wet spell ensues, while, an out-of-phase circulation spells a dry period (as in Figures 45.27d, e and f) of the monsoon.

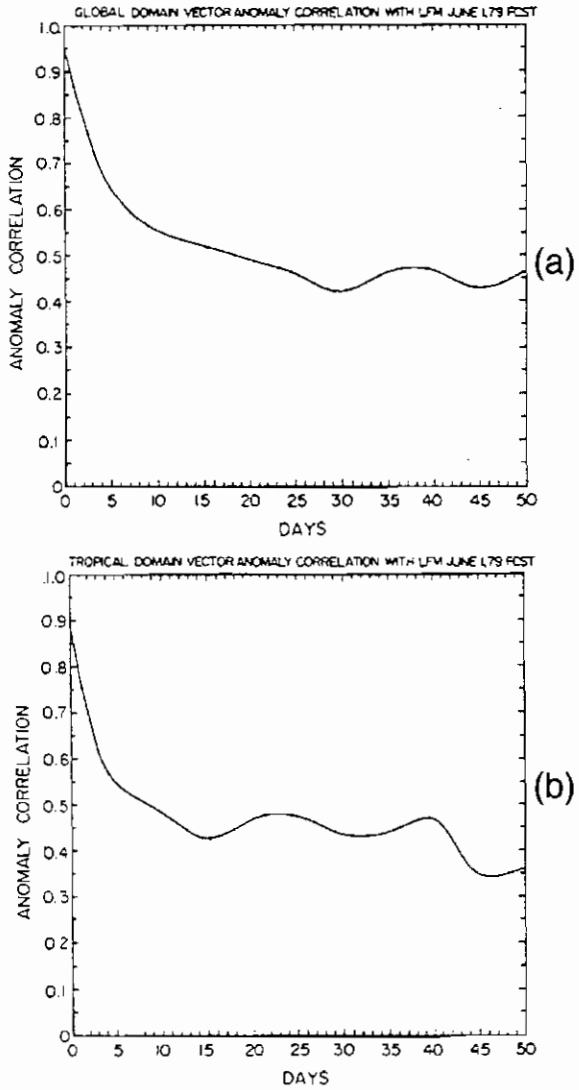

Figure 45.26 Typical anomaly correlations of (a) global and (b) tropical low-frequency component of 850 hPa wind (From Krishnamurti *et al.* 1992b)

Qualitatively such a skill was also noted from the use of ship observations along the heavily traversed lanes connecting Sri Lanka and Sumatra, which were analyzed by Cadet and Daniel (1988). They noted a strong predictive potential from the phase and amplitude of the 30–50-day oscillation along this lane and the subsequent occurrences of dry and wet spells of the monsoon. This was more in the nature of an extrapolative forecast suggesting that one cycle (i.e. a time scale of around forty days) can be predicted.

INTERANNUAL VARIATIONS

Observational studies (Khandekar 1991) on interannual variation of the summer monsoon suggest that Eurasian snow cover, equatorial eastern Pacific sea surface temperatures (SSTs) and the Southern Oscillation Index (SOI) are closely interlinked. Figures 45.28a, b, c and d, based on Khandekar (1991), illustrate the interannual variation of the monsoon rainfall (June–September), Eurasian snow cover departures between December–February and March–May, and sea surface temperature anomalies (SSTA) over the eastern equatorial Pacific and Southern Oscillation (this refers to a see-saw among the sea-level pressure distributions over the Indian Ocean and the eastern Pacific Ocean on a time scale of roughly 4–6 years), respectively. From this figure it is apparent that the large-scale deficit (surplus) years of the Indian summer monsoon rainfall is associated with heavier (lighter)

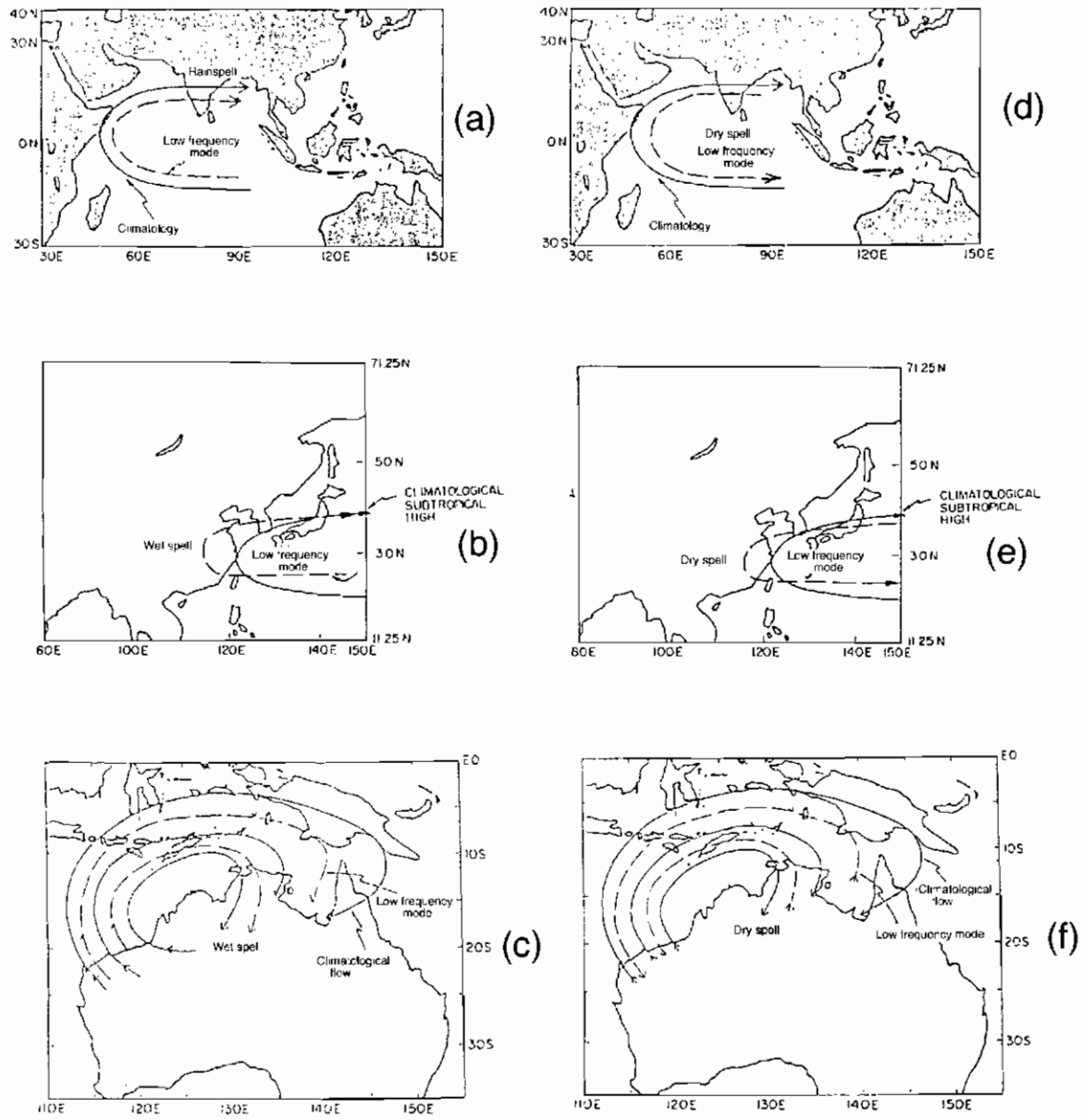

Figure 45.27 Schematic illustration of the low-level flow field for a dry spell over (a) India, (b) China, (c) northern Australia; and wet spell over (d) India, (e) China, (f) northern Australia

than normal Eurasian snow cover during the preceding winter, warmer (cooler) SSTA in the eastern equatorial Pacific and a negative (positive) Southern Oscillation (SO) index. Hahn and Shukla (1976), examining eleven years of satellite-derived winter snow cover over Eurasia and summer monsoon rainfall over India, also observed such an inverse relationship. In addition, Dey and Bhanukumar (1982) noted a direct relationship between spring snow cover over Eurasia and the time taken by the Indian summer

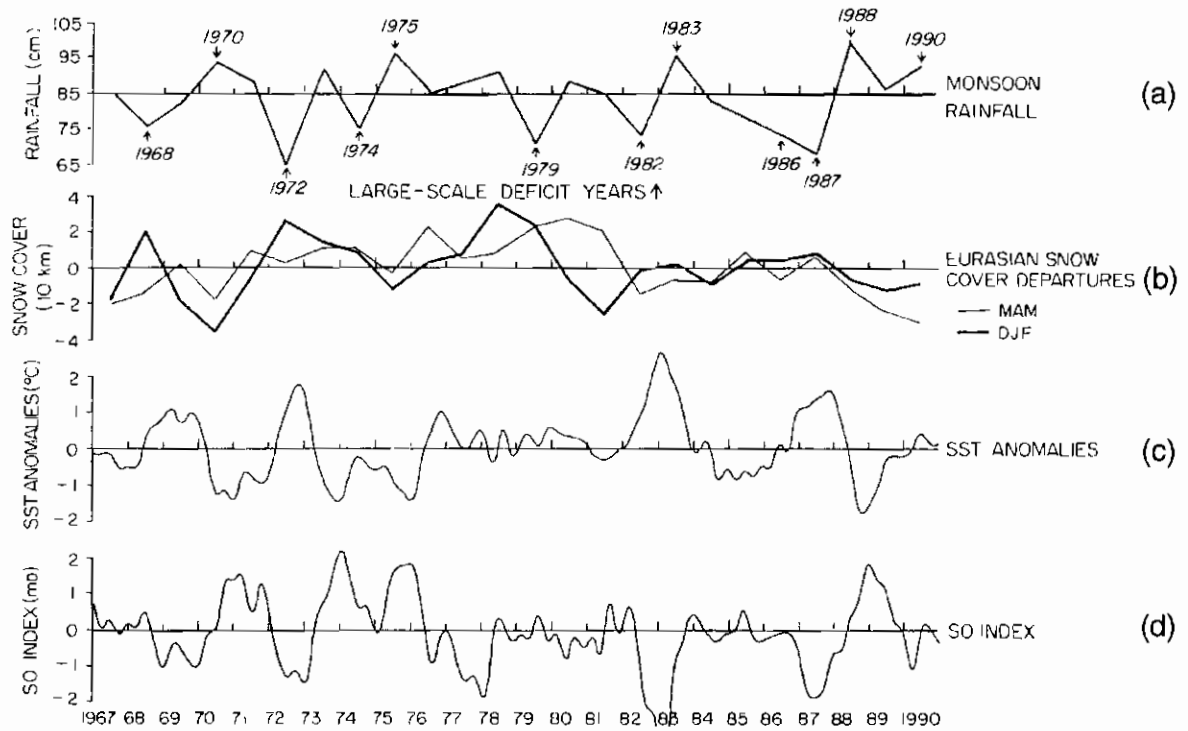

Figure 45.28 Interannual variation in the (a) Indian monsoon rainfall (June–September), (b) the Eurasian snow cover (December–February and March–May) departures, (c) SST anomalies over the area 5°N–5°S, 90–150°W, and (d) the SO index, which is defined as a difference in standardized sea-level pressure between Tahiti and Darwin. The rainfall curve also shows large-scale surplus and deficit years of the Indian monsoon. (From Khandekar 1991)

monsoon rainfall to progress from the southern tip of India to the northern border of India. They report that, for the period 1967–78, the monsoon advanced from the south to the notth much slower when the snow cover in the preceding spring was greater than normal, and vice versa. Such an inverse relationship between the Eurasian snow cover and the progress of summer monsoon rainfall is consistent with the notion that extensive and persistent snow cover has the effect of delaying and weakening the spring and summer heating of the land masses which is necessary for establishing a robust monsoon.

El Niño (Spanish, meaning Christ's child) (i.e. a warm phase of the Southern Oscillation), is a phenomenon which manifests itself as a warm ocean temperature anomaly over the equatorial Pacific Ocean on the time scale of the Southern Oscillation, i.e. roughly four to six years. The events with warmer SST over the eastern equatorial Pacific are generally associated with below-normal Indian summer monsoon rainfall. The creation of a deep tropospheric heat source over the warm SST anomalies is what contributes to the modulation of the planetary-scale phenomenon such as monsoons. The eastward shift of the Walker circulation during El Niño creates large-scale descent upper tropospheric level mass convergence over the Indian monsoon region, influenced by the monsoon rainfall. Rasmussen and Carpenter (1983) have examined the relationship between El Niño events and summer monsoon rainfall over thirty-one Indian climate subdivisions. Figure 45.29 from their study shows the summer monsoon rainfall anomalies (denoted by the bar chart) with negative bars denoting below-normal rainfall years. The dark bars in the figure denote the El Niño events with positive SSTAs over the central and eastern Pacific. From this study, it was noted that from twenty-five El Niño events in the period from 1875 to 1979, the area-averaged Indian

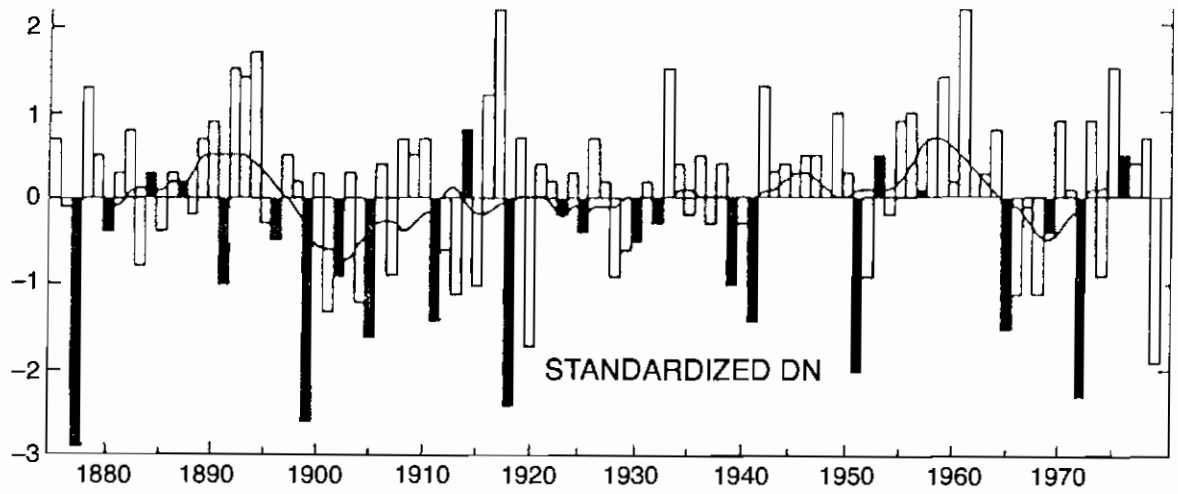

Figure 45.29 A standardized Southern Oscillation index, plotted as a function of years. The dark bars denote those years when there was a strong warm episode (i.e. a strong El Niño year). (Based on Rasmussen and Carpenter 1983)

summer monsoon rainfall was below the median in twenty-one such episodes. However, it should be noted that several years of near normal rainfall are either El Niño or non-El Niño years. Interestingly, correlation studies (e.g. Khandekar 1991) have shown that the SOI and the Indian summer monsoon rainfall exhibit a strong positive correlation (of 0.62) at lag +1 or +2 i.e. SOI variations lead the Indian summer monsoon rainfall by one or two seasons. Shukla and Paolino (1983) plotted the time evolution of the normalized sea-level pressure anomaly over Darwin. This is shown in Figure 45.30. It is apparent from the figure that occurrence of high (low) Darwin pressure anomalies and deficient (heavy) monsoon rainfall anomalies persist for two seasons. The Darwin pressure anomaly decreases in the preceding winter to spring before the heavy rainfall years and increases before deficient rainfall years.

Strong interannual variation of the Indian summer monsoon was observed during the El Niño year of 1987 (Krishnamurti *et al.* 1989) and La Niña (cold phase of the Southern Oscillation) year of 1988 (Krishnamurti *et al.* 1990a). The Indian subcontinent experienced severe drought conditions in June and July of 1987, which under uormal conditions are active monsoon months. The El Niño-related warm sea surface temperatures over the eastern and central Pacific contributed to the eastward and equatorial shift of the planetary-scale divergent circulations in 1987, resulting in large-scale descent over the Indian subcontinent. Furthermore, warm SST anomalies were observed over the near-equatorial southern Indian Ocean, resulting in a southward shift of Hadley-type vertical overturning with descent along roughly 20°S–25°S. In the near-equatorial regions of ascent, a negative anomaly of the stream-function at 850 mb flow was found (Krishnamurti and Surgi 1987). With

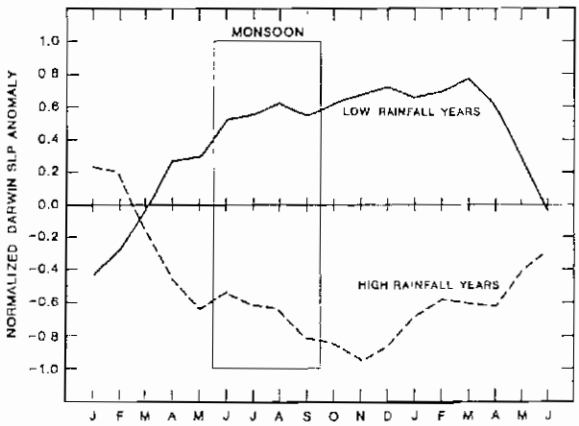

Figure 45.30 Composite of normalized Darwin pressure anomaly (three-month running mean) for heavy monsoon (high) rainfall years and deficient monsoon (low) rainfall years. (From Shukla and Paolino 1983)

the seasonal heating, these anomalies propagated northward across the equator toward central India in July 1987 contributing to a counter-monsoon low-level flow, weakening the southwesterlies. In addition, at 200 mb, negative stream-function anomalies were observed over the Tibetan Plateau. Krishnamurti *et al.* (1989) relate this anomaly to the occurrence of strong westerly winds aloft that entered northwestern India from the dry desert areas of Africa and Arabia and was not simply due to a weakening of the tropical easterly jet. However, in 1988, the warm anomaly in the east and central Pacific disappeared and the Walker Circulation extended westward. In contrast to 1987, a circulation anomaly enhancing the low-level monsoon flow over the Indian subcontinent was observed (Krishnamurti *et al.* 1990a). Furthermore, an easterly anomaly in the stream-function field at 200 mb was also noticed. All of these factors contributed to heavier than normal rainfall over the Indian subcontinent, northeastern China, Japan, the Korean Peninsula and Indo-China.

Verma *et al.* (1985) noted a statistically significant relationship between the Northern Hemisphere surface air temperature and the monsoon rainfall. This statistical relation was most significant with a six-month lag, i.e. warm surface air temperatures over the entire Northern Hemisphere during the winter months are followed by an above-normal summer monsoon rainfall. Joseph *et al.* (1994) have also noted a strong relationship between the Indian monsoon rainfall and the SST variations over the central Arabian Sea near 10°N on the time scale of El Niño. This region is close to the latitude of the Somali jet, where the air–sea exchanges are influenced by the mesoscale (this alludes to scales of the order of few hundred kilometers, this being the typical scale of clustering of cumulo-nimbus clouds) wind speed and SST variations of the order of 10 m s^{-1} and 1°C, respectively.

In El Niño years, two equatorial divergent circulations are prominent, one over the equatorial Indian Ocean and the other over the equatorial central Pacific. As the monsoon proceeds, these two centers merge in the western Pacific Ocean giving rise to a single belt of broad rising motion along the equator from the Indo-China coast to the central Pacific Ocean. However, in La Nina years, the divergent circulation centers are initially located over the equatorial Indian Ocean and the southern Pacific Convergence Zone. These centers move northwards and merge to form a narrow belt of ascent over Indo-China which then moves over to the Bay of Bengal. These equatorial crossings of the divergent circulations, which are also seen in rainfall anomalies, excite a wave train similar to the Pacific North American (PNA) pattern (Krishnamurti *et al.* 1997a). Figures 45.31a and b illustrate such a wave train excited in the Northern Hemisphere in spring and in the Southern Hemisphere in fall from a composite map of the difference in 300 mb heights ten days prior to and after the equatorial crossing. The wave train emanates from the tropics into subtropical and middle latitudes. This is observed to excite a precipitation signature with alternating wet and dry regions along the wave train. The region east of the upper-level trough in the wave train tends to be wet while it is dry to the west of the upper-level trough, resulting in a transient climate over the east China coast.

Gadgil *et al.* (1993) noted large regional differences in intraseasonal climate. Based on these findings they defined some thirty-one coherent rainfall zones over India based on high intercorrelation of the rainfall time series of weather reporting sites within each of the (thus defined) zones. In order to define these thirty-one distinct zones, they utilized an initial database from 200 sites. This definition of coherent zones provides an array for long-term climate studies of the monsoon on seasonal and longer time scales.

In a detailed empirical study using nine years of snow cover and the Indian monsoon rainfall datasets, Kripalani *et al.* (1996), noted a very strong inverse relationship between the snow mass during January, over a region northeast of Moscow and over Mongolia and Siberia, and the subsequent summer monsoon rain over India. These observations have been exploited in the statistical and modeling studies of seasonal forecasts by many scientists.

The India Meteorological Department, Gowarikar *et al.* (1991), has developed a statistical regression method for long-range (three to six months in advance) monsoon forecasts. This regression includes several parameters such as: 10 mb westerly winds over Balboa (Quasi-biennial Oscillation refers to a period close to two years, closer to twenty-six months; this phenomenon is most conspicuously noticed over the

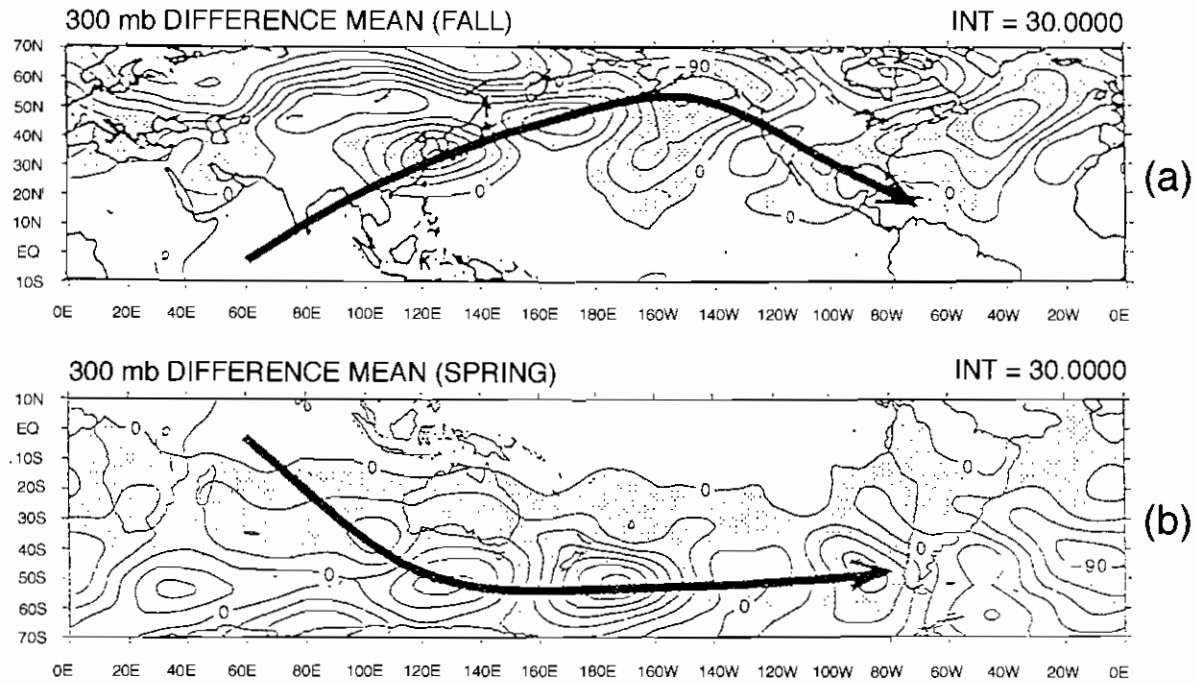

Figure 45.31 (a) Illustrates the northward passage of the 300 mb geopotential anomalies from six cases. The contour interval is 30 gpm. Shaded regions represent negative values. The solid arrow represents the wave train. This is based on Krishnamurti *et al.* (1997). (b) As in Figure 45.31a except for southward passage of the geopotential anomalies

equatorial lower stratosphere where the zonal winds alternate between westerlies and easterlies globally at this time scale); pressure during April over Darwin; the Eurasian snow cover during the previous December; mean pressure over the equatorial Indian Ocean during January through May; Himalayan snow cover during January through March; surface air temperature averaged over central India during May; 500 mb ridge over central India during January and February; monthly mean minimum temperature over northern India during March; the minimum temperature over the east coast of India during March; mean surface air temperature over the Northern Hemisphere during January and February; and the Southern Oscillation index and pressure over Argentina during April. Statistical forecasts are issued prior to the start of the summer monsoon season each year. These have been quite promising for nearly a decade. In 1997, in spite of an early El Niño onset, this method predicted near normal rain over India; it would be interesting to see if this is verified.

The AMIP (Atmospheric Model Intercomparison Project, 1995) was aimed at examining the relative performance of several global models. These are global atmospheric general circulation models where the sea surface temperatures are prescribed. The monsoon simulations from these models were studied by Gadgil and Sajani (1997). Figure 45.32a, b, c, d, e and f show the observed seasonal mean results from the different models. Here we present seasonal mean precipitation simulations of the winter and the summer monsoon. As is clearly evident, the seasonal mean rainfall from the different models shows almost no mutual agreement, or any agreement with observations. Rains have occurred here, there and anywhere. This is considered an important result by several scientists, who attribute these differences to the large internal variability of the monsoon forecasts and they infer that these internal variabilities overwhelm the slow surface forcing from the SSTs and the snow cover. These are issues that deserve further studies. Some pessimism has been expressed by a few climate

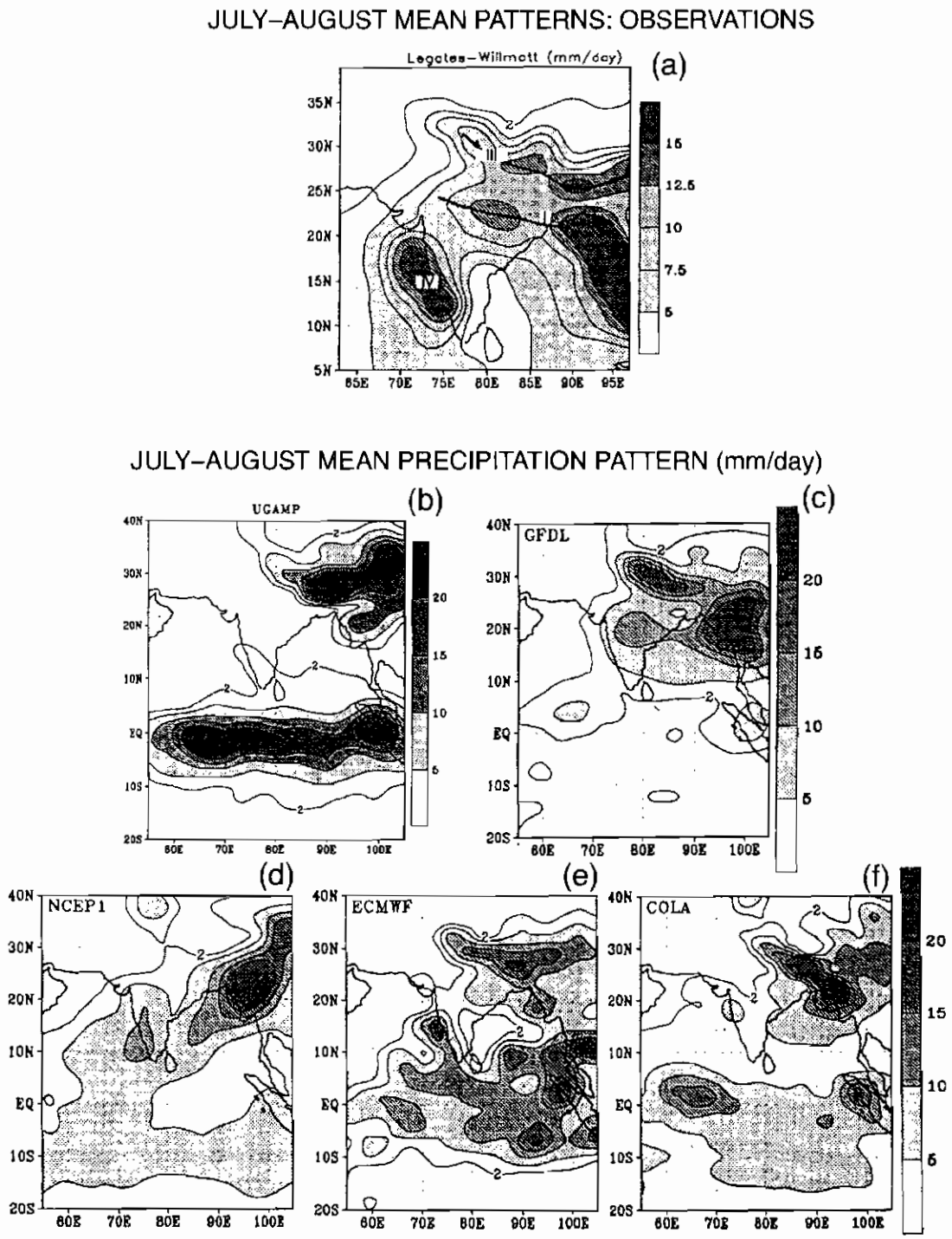

Figure 45.32 (a) Observed mean (for the AMIP period) July–August precipitation. (b) Typical pattern of formulation of the mean July–August precipitation for UGAMP. (c) Same as (b) but for GFDL. (d) Same as (b) but for NCEP1. (e) Same as (b) but for ECMWF. (f) Same as (b) but for COLA

modelers who now feel that seasonal forecasts of monsoon may have to be done using the statistical methods. However, it is possible that all of these are relatively low-spatial resolution climate models and they do not resolve the organization of convection needed to drive the monsoon. The coupling of the lower boundary conditions to the atmosphere occurs via this organized convection which simply needs a higher resolution. Very high resolution data assimilation with physical initialization within a coupled atmosphere–ocean model appears to offer some hope for further improvement of seasonal forecasts.

CLIMATE MODELING OF THE MONSOONS

Seasonal simulations of the monsoon have shown that SST, land surface parameterization, initial conditions, detailed orography and the resolution of the model are extremely important. Palmer *et al.* (1992) conducted several sensitivity studies to examine the impact of regional SST anomalies on seasonal forecasts of the monsoons. Their study revealed that interannual differences in rainfall forecasts over the Sahel and India between 1987 and 1988 were associated almost entirely with tropical Pacific SST anomalies while the Indian Ocean did not exhibit such an influence. Summer seasonal mean rainfall over the Sahel, East Africa, India and south Indian Ocean observed an enhancement in 1988 relative to 1987 when the west Pacific Oceau exhibited warmer SST anomalies. However, anomalies in the Indian and Atlantic Oceans indicated a more passive response to the interannual monsoon variability. Observational studies such as Shukla and Paolino (1983) have also suggested that the Indian monsoon rainfall is correlated more strongly with Pacific SST anomalies than with Indian Ocean SST anomalies. Simulation studies with the Center for Ocean–Land–Atmospheric (COLA) Studies model (Fennessy 1993) suggested a strong correlation of the interannual differences in the monsoon precipitation of 1987 and 1988 with the intraseasonal differences. This is illustrated in Figures 45.33a and b. Primarily, the wet and dry spells in a monsoon season are related to the fluctuation of the regional tropical convergence zone with its favorable location being either over the subcontinent (continental regime) or over the equatorial Indian Ocean (oceanic regime), respectively (Goswami 1993). Palmer (1993) noted from these observations that the El Niño SST anomalies might influence the probability of occurrence of the continental regime or the oceanic regime, though the regime structure itself would be relatively unaffected by the SST anomalies. Furthermore, the author suggests that prediction of the time spent in one regime relative to others is highly uncertain. This warrants a design of an ensemble of integrations to assess the impact of SST anomalies on regime residence statistics.

In studying the impact of initial conditions to seasonal simulations of the monsoons, Palmer *et al.* (1992) designed two experiments with a T42 version of the ECMWF model. These model runs were three-month integrations with identical SSTs but initial conditions one day apart. The experiments showed that the large-scale velocity potential (this is a scalar potential filed whose gradient provides the direction and strength of the divergent wind) and stream-function was predominated by the impact of anomalous ocean forcing rather than variations in the initial state. This observation is consistent with the work of Charney and Shukla (1981) which emphasized that the predictability of monsoons arises in part due to relative insensitivity of the large-scale atmospheric circulation in the tropics to the initial conditions in comparison with its dependence on boundary conditions. However, regional rainfall, particularly over parts of India and Southeast Asia, indicated high sensitivity to initial conditions. Ji and Vernekar (1997) simulated the interannual variation of the Asian monsoon using a nested high-resolution grid point model with a horizontal resolution of 80 km with prescribed SST, snow cover and soil moisture. Their study revealed that a significant fraction of total precipitation in the Asian monsoon region is due to deep convection associated with the orography of the region which generate mesoscale circulations. Seasonal monsoon forecasts contrasting the below-normal monsoon rainfall season of 1987 and the above-normal rainfall of 1988 were studied by several authors, in particular by Laval *et al.* (1996). They used an atmospheric global circulation model (GCM), a variable spatial resolution grid point global model. The key issue contrasting these rainfall features of the El Niño year, 1987, and the La Niña year, 1988, were

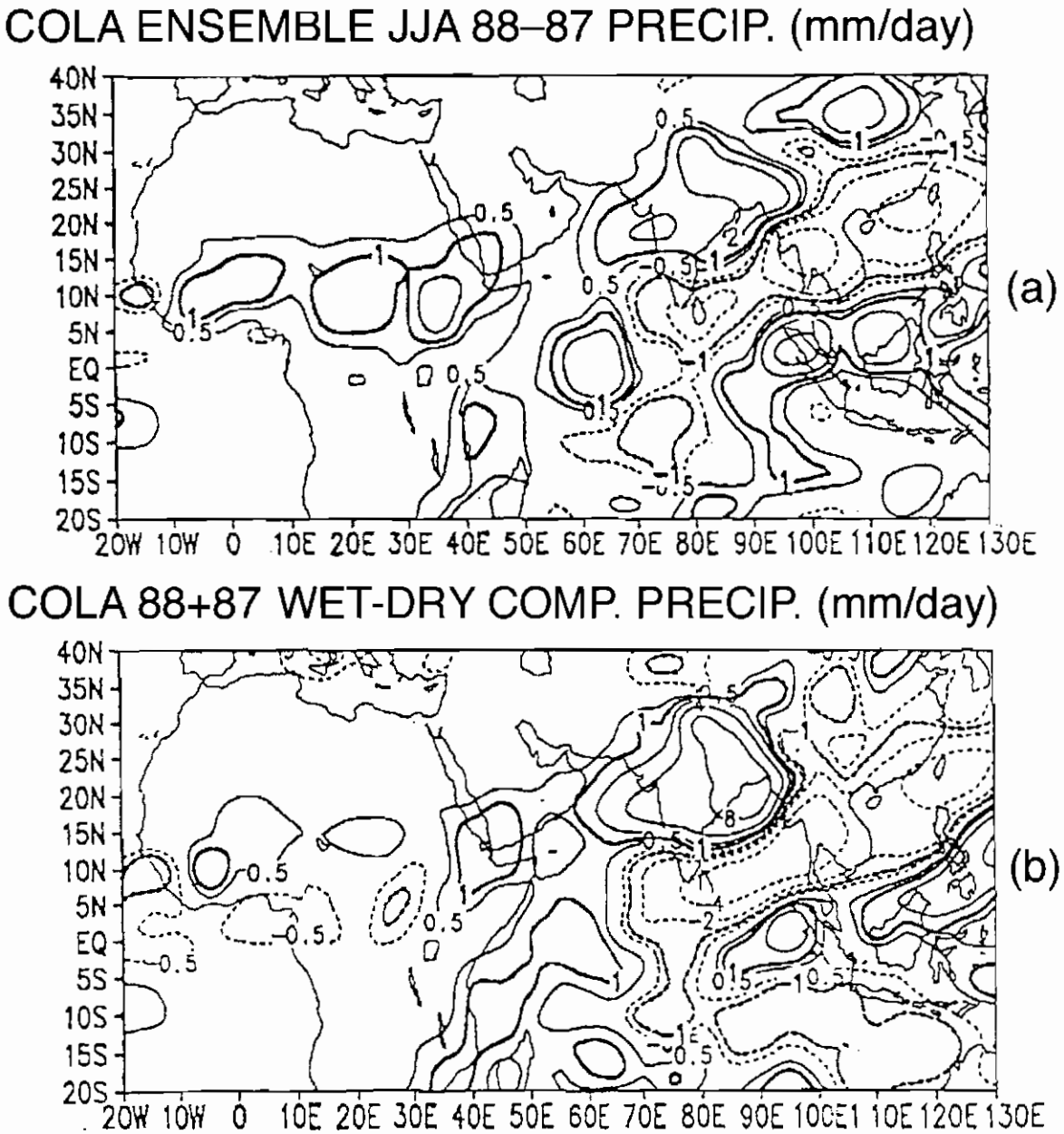

Figure 45.33 (a) Ensemble mean JJA difference rainfall between 1988 and 1987 MONEG integrations of the COLA model. (b) Composite difference between active and break periods of the monsoon from within the COLA–MONEG integration. This is based on Fennessy (1993)

the land surface properties, i.e. the soil moisture. Although the Pacific Ocean SST were quite dissimilar during these years the Indian Ocean SSTs were closer to each other. This was also noted by Dumenil (1993). The dryness of the soil during the spring months of 1987 was noted as a primary contributor to the extension of the dryness. Fennessy (1993) noted that there is a strong tendency for better

seasonal mean precipitation simulations with increasing resolution. The most obvious improvement obtained with increasing resolution was a better simulation of the maxima on either coast of the Indian subcontinent. In reality, much of the observed tropical rainfall is in response to transients on small spatial and temporal scales which most climate models have difficulty in simulating. Furthermore, these transients are dynamically coupled to the planetary scale flow in the tropics (Palmer *et al.* 1992). Imperfect simulation of such transient features in the model reflects that the rainfall variability is not well coupled with the simulated planetary scale flow which might be a consequence of several deficiencies in the model. Experiments on the sensitivity of the monsoon behavior to the variations of Eurasian snow cover have been investigated by Vernekar *et al.* (1995). Basically the well-known inverse relationship, i.e. larger extent and depth of Eurasian snow cover in the spring months to a reduction of monsoon seasonal rainfall, was verified by this modeling experiment.

Krishnamurti *et al.* (1995b) illustrated an improved simulation of the interannual variation of the Asian summer monsoon with an advanced ground wetness parameterization (Bounoua and Krishnamurti 1993a, 1993b) which is based on the surface energy balance method. This parameterization is a function of a number of fixed and time-dependent parameters, the most important of which is the past rainfall. In analyzing the contrasting behavior of the 1987 and 1988 summer monsoon from such a model, Krishnamurti *et al.* (1995b) found from the residue-free moisture budget studies that the excess rainfall in 1988 over the region arose from a larger net convergence of moisture, produced by enhancement of evaporation in the Indian Ocean and the Arabian Sea.

PARTITIONING A SEASONAL MONSOON SIMULATION

It is possible to carry out a residue-free budget of a model's seasonal mean simulation for any of its basic variables. For instance, one could ask why a seasonal simulation resulted in a certain anomaly of a time-mean geopotential height (this denotes the height of a pressure surface above sea level) at any vertical pressure level of the model atmosphere. This type of partitioning for a non-linear climate model was proposed by Krishnamurti *et al.* (1996). Here, several processors of a supercomputer carry the history of the tendencies of a reference variable arising from different portions of the model's physics and dynamics. As an example we could ask what are the contributions to a seasonal mean geopotential height anomaly at 500 mb from factors such as:

1 non-linear advective dynamics in the model;
2 linear dynamics;
3 air–sea interaction;
4 land surface processes;
5 deep cumulus convection;
6 large-scale non-convective precipitation;

and other such features of a comprehensive model.

A central processor carries the full model, whereas the other processors borrow the final results at the end of each time step from the central processor and carry out a one time-step integration suppressing one of the above factors. This procedure merely provides the bookkeeping for a residue-free budget and can address the budget (i.e. model contribution) from any part of the model.

Using this approach several questions were asked in relation to the behavior of the simulated monsoon for the years 1987 and 1988: 1987 was an El Niño year and 1988 a La Niña year. The 200 mb Tibetan anti-cyclone complex migrated westwards and northwards between these respective years by roughly 5° longitude westward and 5° latitude northwards. The residue-free budgets were used to ask which of the forcings were important for this eastward migration.

The qualitative explanation for this shift is usually ascribed to the warm SST anomaly of the equatorial central Pacific Ocean, which results in a shift of convection eastward during an El Niño year. This is usually accompanied by a shift of the divergent circulations. The descending branch of these east–west circulations are often located over the Asian landmass, resulting in below-normal monsoon rainfall activity (Kanamitsu and Krishnamurti 1978; Rasmussen and Carpenter 1982). Descending air over the Asian landmass results from upper-tropospheric convergence; the resulting generation of cyclonic vorticity weakens the Tibetan anticyclone and this contributes to this eastward shift, the upper tropospheric high over the

Pacific being maintained by the El Niño convection. We shall next examine the results of seasonal climate forecasts on the tendencies of 200 mb geopotential heights over Africa and Asia to assess what were the salient dynamical and physical components of the model that contributed to this eastward shift in model simulations.

The model-based seasonal buildup of the 200 mb high over the African–Asian belt was higher in 1988 than 1987. Largely, that buildup is attributed to dynamical contributions, among which the advective dynamics tended to lower the height of the 200 mb surface over this area much more during 1987 than 1988. In the model, this contribution from advective dynamics is counteracted by the other dynamics, with the largest contribution coming from the divergence terms of the vorticity equation. The effect of this term in both years was to increase the 200 mb height. The height changes by advective dynamics during 1987 were more negative than those during 1988. This is attributed to upper-troposphere convergence over the Asian–African region related to the downward branches of east–west circulations, which contributed to a generation of vorticity and a lowering of heights during the El Niño year. The effect is offset by an increase in height by the rest of the dynamics.

It should be noted that we are comparing geopotential height tendencies for an entire season, where the tendency implies the geopotential height difference between August 31 and June 1 for the respective years. For both years, on June 1 the mean height of the 200 mb was in fact smaller than that on August 31. The change was less positive in 1987 compared to that during 1988; the seasonal height change in 1988 (the above-normal monsoon rainfall year) was less negative because of the contributions of non-advective dynamics. The direct contributions from physics towards the height tendencies over this large domain were not all that different during the two years. Convective heating contributed to an elevation of the 200 mb heights, non-convective heating contributed much less. The radiative effects in both years contributed to a net lowering of the 200 mb surface. Overall, there was a basic cancellation of the tendencies from the convective and radiative contributions. The contributions from the total physics were smaller than those from the dynamics over this selected domain.

The main issue is that of the eastward shift of the upper anticyclone in 1987 with respect to its position in 1988. Excessive upper-level convergence in the El Niño year 1987, arising from the divergent circulation, appears to be the primary contributor for the generation of cyclonic vorticity at the upper levels of the monsoon, resulting in the lowering of the heights. The eastward shift of the upper anticyclone appears to be more directly related to changes in the planetary-scale divergent circulations related to El Niño. The direct effects from changes in local heat sources appear to be insignificant for these height changes.

In summary, we find that deep convection over the central Pacific contributed to a general descent via east–west circulation over the regions of the African–Asian monsoon. An eastward shift of the Tibetan anticyclone is mainly attributed to the descent, the upper tropospheric mass convergence and the generation of cyclonic vorticity over this region. This is what we had expected from our synoptic experience.

The contributions to the 500 mb seasonal mean forecasts of the geopotential height averaged between 30° and 40°N, for the longitude belt 30°–150°E during the 1988 monsoon season are illustrated in Figure 45.34. This was the post-El Niño year with above-normal rainfall over the Indian subcontinent. We display the breakdown of the contributions to the predicted mean height from the components of the model's history. The contributions from total dynamics and total physics (Figure 45.34) show that over the Asian monsoon domain, between roughly 50° and 110°E, the contribution of physical processes is to elevate the 500 mb surface well above the final predicted value. The contribution from the total dynamics lowers the heights over this region. The two processes evolve to counteract each other. The magnitude of these two processes is substantial, that is, on the order of 40 m. The issue is whether something can be said about the role of dynamics in the seasonal mean height. It is clear that dynamical contributions are indeed very large. When one partitions the dynamical contributions into those arising from advective non-linearity and those from the rest of the dynamics (Figure 45.34c), we note that this large total dynamical contribution is again composed of two opposing contributions, that is, from the non-

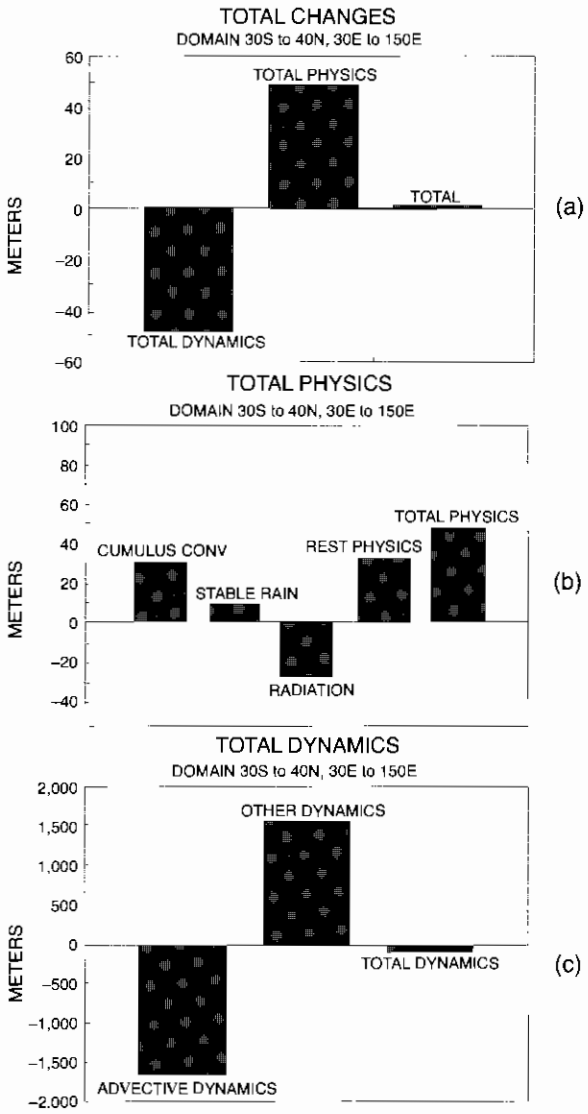

Figure 45.34 The 500 mb seasonal height tendency for the summer of 1988 over the domain 30°S–40°N, 30°–150°E. (a) Contributions from total physics and total dynamics, (b) contributions from physical processes, and (c) contributions from dynamical processes

linear advective dynamics (this denotes the role of non-linear terms in the dynamical equation of the system being considered here) and the rest of dynamics. The advective dynamics tends to lower the 500 mb geopotential substantially; that is, advective non-linearities contribute to negate the final seasonal mean state. The total contributions from dynamics are in fact comparable to magnitudes of the individual contributions from the various physical processes, as illustrated in Figure 45.34b. Cumulus convection, by far, contributes the most to elevate the 500 mb geopotential surface over the monsoon region. That is partly offset by the radiative contributions. Large-scale condensation heating, in this instance, appears to elevate the 500 mb surface. The air–sea and land–air interactions (and resulting vertical convergences of fluxes) contribute to a net elevation of the 500 mb surface as well.

In the end, when examining the magnitudes of these various components, we note that advective non-linearities, the rest of the dynamics, and cumulus convection by far share the largest contributions in shaping the final 500 mb seasonal mean geopotential height over the monsoon region.

CONCLUDING REMARKS AND FUTURE OUTLOOK

Monsoon research has moved on from the more descriptive and modeling aspects of the onset, active and break scenarios to the areas of intraseasonal and interannual variabilities. Much progress has been seen in recent decades in the observational and simple modeling of these time scales. A large number of scientific papers have examined the role of surface boundary conditions, including sea surface temperatures, snow cover and albedo. It is also being recognized that the slow variability of these lower boundary conditions do not simply provide a verifiable slow variability of the monsoon. The slow variability of the monsoon on the intraseasonal and especially the interannual time scales appears to be also a function of the strong internal chaotic variability of the atmosphere (Ferranti *et al.* 1997). In this important study with the AMIP global models (which ran for ten years along prescribed SSTs) it was clearly noted that the dominant mode of variability of the monsoon showed only a weak level of reproducibility compared to the observed monsoon. This provides a major challenge for future modeling. Our studies on monsoon prediction (Krishnamurti *et al.* 1998b) place a major emphasis on the resolving of the organization of convection for monsoon forecasts.

Most climate models, coupled or uncoupled, utilize resolutions of the order of T42 with some exceptions (such as Ferranti *et al.* 1997, who use a resolution of T106). At these resolutions the monsoon convection is not organized on the scales of the monsoon disturbances. Energetically the maintenance of the monsoon shifts from a disturbance adapted to a local Hadley cell-oriented scale, that simulates large planetary-scale characteristics of the monsoon, but fails to have a skill in predicting monsoon disturbances on the medium range. (The Hadley cell is a well-known slow vertical and north–south circulation of a zonally averaged motion field. This circulation exhibits slow rising air in the near 30°N or 30°S latitudes.) Using a resolution of T255 it is possible to pass on the satellite rainfall at the resolution of its footprint to the transform grid resolution of the model. Physical initialization, thus carried out, appears to handle the mesoconvective precipitation structures of monsoon disturbances in a more realistic manner than lower resolutions do. There still remains the strong possibility that the organization of monsoon convection provided by high-resolution models (as seen in medium-range forecasts) is what is required to provide the needed link between the slow forcing of the surface boundary conditions and the evolution of the intraseasonal and the interannual monsoon climate. Lacking such an organization we lose the integrity of most monsoon disturbances that are essential elements for defining the monsoon climate!

This raises the following issue: do we need to resort to higher-resolution climate models for monsoon simulations, or do we need to parameterize the organization of convection in some innovative ways for lower-resolution models? This current bias in lower resolution models is a north–south flow catastrophe that tends to slowly degrade the divergent north–south flows in favor of more non-divergent east–west flows on disturbance scales. As a consequence we often see an almost total lack of monsoon disturbances. Some semblance to monsoon-like circulations in lower-resolution models arises largely from a description of the differential heating related to orographic and larger-scale rainfall features. However, the above argument certainly does not rule out the possibility that climate modeling at high resolutions would cease to exhibit chaotic behavior. Further modeling work is clearly needed to address these issues.

The statistical (regression) approach, being pursued in India for seasonal forecasts of monsoon rainfall has performed reasonably well over the last six years. This makes use of some fifteen or so antecedent parameters (from the season before) to predict a single number, an index, for monsoon rainfall over the whole country. This approach has not succeeded in providing regional skill which varies from one region to another and rather drastically from one season to the next. It is not clear whether the future modeling will be entirely statistical, nor is it apparent that a mix of statistical and deterministic approaches needs to be pursued. Further work is apparently needed in both areas.

Going through the monsoon literature, we have noted that a vast amount of "monsoon facts" reside in numerous published and unpublished literature. These dwell on many space–time scales of the monsoon. A clearer synthesis of that literature is currently lacking. This includes many findings especially in the smaller scales which we believe have an impact on our understanding of the larger space–time scales. Future work on the synthesis of this material is extremely important; much of this literature resides in India and China.

ACKNOWLEDGMENTS

The research reported here was supported by NASA grant no. ATM-9312537, NOAA grant no. NA16RCO358-02, and NSF grant no. ATM-9312537.

LIST OF ACRONYMS

AMIP	Atmospheric Model Intercomparison Project
COLA	Center for Ocean–Land–Atmosphere Studies
ECMWF	European Centre for Medium-range Weather Forecasts
ENSO	El Niño Sourhern Experiment
FGGE	First GARP Global Experiment
FSU	Florida State University
GARP	Global Atmospheric Research Project

GCM	Global Circulation Model
GFDL	Geophysical Fluid Dynamics Laboratory
INDOEX	Indian Ocean Experiment
ITCZ	Intertropical Convergence Zone
KE	Kinetic energy
MONEG	Monsoon Numerical Experimentation Group
MONEX	Monsoon Experiment
NCEP	National Center for Environmental Prediction
OLR	Outgoing longwave radiation
PNA	Pacific North American
Q_1	Apparent heat source
Q_2	Apparent moisture sink
QBO	Quasi-biennial Oscillation
SO	Southern Oscillation
SOI	Southern Oscillation Index
SSM/I	Special sensor microwave imager
SST	Sea surface temperature
SSTA	Sea surface temperature anomaly
T21, 31, 42, 63, 106, 170 and T255	Triangular truncation at wave numbers 21, 31, 42, 63, 106, 170 and 255
TIROS	Television and infrared operational satellite
UGAMP	UK Universities Global Atmospheric Modelling Project
UTC	Universal time coordinated

REFERENCES

Ackerman, S.A. and Cox, S.K. (1982) "The Saudi Arabian heat low: aerosol distribution and thermodynamic structure", *J. of Geophysical Research* 87: 8991–9002.

Ackerman, S.A. and Chuug, H. (1992) "Radiative effecrs of airborne dust on regional energy budgets ar the top of the atmosphere", *J. Appl. Meteor.* 31: 223–33.

Ardauuy, P. (1979) "On the observed diurnal oscillations of the Somali jet", *Mon. Wea. Rev.* 107: 1694–700.

Asnani, G.C. (1993) *Tropical Meteorology*, Vols 1 and II. Printed by Noble Printers, Pune, India.

Bounoua, L. and Krishnamurti, T.N. (1993a) "Influence of soil moisture on the Sahelian climate prediction – Part 1", *J. Meteor. Atmos. Phys.* 52: 183–203.

Bounoua, L. and Krishnamurti, T.N. (1993b) "Influence of soil moisture on the Sahelian climate predicrion – Part II", *J. Meteor. Atmos. Phys.* 52: 205–24.

Cader, D. (1983) "The monsoon over the Indian Ocean during summer 1975. Part 11: hreak and acrive monsoons", *Mon. Wea. Rev.* 111: 95–108.

Cadet, D. and Daniel, P. (1988) "Long-range forecasr of the break and active summer monsoons", *Tellus* 40A: 133–50.

Carlson, T.N. and Benjamin, S.G. (1980) "Radiarive heating rates for Saharan dusr", *J. Atmos. Sci.* 37: 193–213.

Chang, C.P. and Krishnamurti, T.N. (1987) "Monsoon mereorology", *Oxford Monographs of Geology and Geophysics*, no. 7.

Charney, J.G. (1975) "Dynamics of deserts and drought in the Sahara", *Quart. J. Roy. Meteor. Soc.* 101: 193–202.

Charney, J.G., and Shukla, J. (1981) "Predictability of monsoons", *Monsoon Dynamics*, J. Lighthill and R. Pearce (eds), Cambridge University Press, Cambridge.

Chen, T.C. and Weng, S.P. (1996) "Some effects of the inrraseasonal oscillation on the equatorial waves over the western tropical Paeific–South China Sea region during the northern summer", *Mon. Wea. Rev.* 124: 751–56.

d'Almeida, G.A. (1987) "On the variability of desert aerosol radiative characteristies", *J. Geophys. Res.* 92: 3017–26.

Davidson, N.E. (1995) "Vortieity budget for AMEX. Part II: simulations of monsoon onset, midtroposphcric lows, and tropical cyclone behavior", *Mon. Wea. Rev.* 123: 1636–59.

Dey, B. and Bhanukumar, O.S.R.U. (1982) "An apparent relationship between Eurasian spring snow cover and the advance period of the Indian summer monsoon", *J. Appl. Meteor.* 21: 1929–32.

Dumenil, L. (1993) "Simulation and prediction of monsoons: recent results", WMO/TD, No. 546. New Delhi, India, March.

Fennessy, M. (1993) "MONEG related research at COLA", WMO/TD, No. 546. Simulation and prediction of monsoons: reecnt results, New Dehli, pp. 19–22.

Ferranti, L., Slingo, J.M., Palmer, T.N. and Hoskins, B.J. (1997) "Relations between interannual and intraseasonal monsoon variability as diagnosed from AMIP integrations", *Quart. J. Roy. Meteor. Soc.* 123: 1323–57.

Gadgil, Sulochana, Yadumani and Joshi, N.V. (1993) "Coherenr rainfall zones of the Indian region", *J. Climate* 13: 547–66.

Gadgil, S., Sajani, S. and participating modeling groups of AMIP (1997) "Atmospheric Model Intercomparison Project (AMIP). Monsoon precipitation in the AMIP runs (resulrs from an AMIP diagnostic subproject)", Centre for Atmospheric and Oceanic Schemes, I.I.Sc., Bangalore, 560012, India.

Gairola, R.K. and Krishnamurti, T.N. (1992) "Rain rates based on SSM/I, OLR and raingauge data sets", *Meteor. Atmos. Phys.* 150: 165–74.

Gill, A.E. (1980) "Some simple solutions for hear-induced

tropical circulation", *Quart. J. Roy. Meteor. Soc.* 106: 447–62.

Gill, A.E. and Philips, P.J. (1986) "Nonlinear effects on heat-induced circulation of the tropical atmosphere", *Quart. J. Roy. Meteor. Soc.* 110: 69–91.

Goswami, B.N. (1993) "Deterministic non-periodic flow", *J. Atmos. Sci.* 42: 433–71.

Gowarikar, V., Thapliyal, V., Kulshrestha, S.M., Mandal, G.S., Sen Roy, N. and Sikka, D.R. (1991) "A power regression model for long range forecast of southwest monsoon rainfall over India", *Mausam* 42: 125–30.

Grossman, R.L. and Duran, D.R. (1984) "Interaction of low-level flow with the western Ghat mountains and offshore convection in the summer monsoon", *Mon. Wea. Rev.* 112: 652–72.

Hahn, D. and Shukla, J. (1976) "An apparent relationship between Eurasian snow cover and Indian monsoon rainfall", *J. Atmos. Sci.* 33: 2461–63.

Hartmann, D.L. and Michelsen, M.L. (1989) "Intraseasonal periodicities in Indian rainfall", *J. Atmos. Sci.* 46: 2838–62.

Hayashi, Y. (1980) "Estimation of nonlinear energy transfer spectra by the cross-spectral method", *J. Atmos. Sci.* 37: 299–307.

Ji, Y. and Vernekar, A.D. (1997) "Simulation of the Asian summer monsoons of 1987 and 1988 with a regional model nested in a global GCM", *J. Climate*, in press.

Joseph, P.V., Eischeid, J.K. and Pyle, R.J. (1994) "Interannual variability of the onset of the Indian summer monsoon and its association with atmospheric features, El Niño, and sea surface temperature anomalies", *J. Climate* 7: 81–105.

Joshi, P.C., Simon, B. and Desai, P.S. (1990) "Atmospheric thermal changes over the Indian region prior to the monsoon onset as observed by satellite sounding data", *International J. of Climatology* 10: 49–56.

Kanamitsu, M. and Krishnamurti, T.N. (1978) "Northern summer tropical circulation during drought and normal rainfall months", *Mon. Wea. Rev.* 106: 331–67.

Khandekar, M.L. (1991) "Eurasian snow cover, Indian monsoon and El Niño/Southern Oscillation – a synthesis", *Atmosphere – Ocean* 29: 636–47.

Kripalani, R.M., Singh, S.V., Vernekar, A.D. and Thapliyal, V. (1996) "Empirical study on nimbus of snow mass and Indian summer monsoon rainfall", *International J. of Climatology* 16: 23–34.

Krishnamurti, T.N. (1978) "Monsoon dynamics. Contributions to current research", in *Geophysics*, Birkhauser Verlag, pp. 1087–529.

Krishnamurti, T.N. and Ramanathan, Y. (1982) "Sensitivity of the monsoon onset to differential heating", *J. Atmos. Sci.* 39: 1290–306.

Krishnamurti, T.N. and Subramaniam, D. (1982) "The 30–50 day mode at 850 hPa during MONEX", *J. Atmos. Sci.* 39: 2088–95.

Krishnamurti, T.N. and Surgi, N. (1987) "Observational aspects of summer monsoon", in *Monsoon Meteorology*, C.P. Chang and T.N. Krishnamurti (eds), Oxford University Press, Oxford, pp. 3–25.

Krishnamurti, T.N. and Bedi, H.S. (1988) "Cumulus parameterization and rainfall rates: Part III", *Mon. Wea. Rev.* 116: 583–99.

Krishnamurti, T.N., Pan, H., Chang, C.B., Polsney, J. and Oodally, W. (1979) "Numerical weather prediction for GATE", *Quart. J. Roy. Meteor. Soc.* 105: 979–1010.

Krishnamurti, T.N., Bedi, H.S. and Subramaniam, M. (1989) "The summer monsoon of 1987", *J. Climate* 2: 321–40.

Krishnamurti, T.N., Bedi, H.S. and Subramaniam, M. (1990a) "The summer monsoon of 1988", *J. Meteor. Atmos. Phys.* 42: 19–37.

Krishnamurti, T.N., Subramaniam, M., Oosterhof, D. and Daughenbaugh, G. (1990b) "On the predictability of low-frequency modes", *J. Meteor. Atmos. Phys.* 44: 63–84.

Krishnamurti, T.N., Xue, J., Bedi, H.S., Ingles, K. and Oosterhof, D. (1991) "Physical initialization for numerical weather prediction over the tropics", *Tellus* 45A: 247–69.

Krishnamurti, T.N., Sinha, M.C., Krishnamurti, R., Oosterhof, D. and Comeaux, J. (1992a) "Angular momentum, length of day and monsoonal low-frequency mode", *J. Meteor. Soc. Japan* 1B: 131–66.

Krishnamurti, T.N., Subramaniam, M., Daughenbaugh, G., Oosterhof, D. and Xue, J. (1992b) "One month forecasts of wet and dry spells of the monsoon", *Mon. Wea. Rev.* 120: 1191–223.

Krishnamurti, T.N., Han, S.K. and Vasubandhu Misra (1995a) "Prediction of the dry and wet spell of the Australian monsoon", *J. Climatology* 15: 753–71.

Krishnamurti, T.N., Bedi, H.S., Rohaly, G., Fulakeza, M., Oosterhof, D. and Ingles, K. (1995b) "Seasonal monsoon forecast for the years 1987 and 1988", *Global and Planetary Change* 10: 79–95.

Krishnamurti, T.N., Bedi, H.S., Rohaly, G.D. and Oosterhof, D. (1996) "Partitioning of the seasonal simulation of a monsoon climate", *Mon. Wea. Rev.* 124: 1499–519.

Krishnamurti, T.N., Wagner, C.P., Cartwright, T.J. and Oosterhof, D. (1997a) "Wave trains excited by cross-equatorial passage of the monsoon annual cycle", *Mon. Wea. Rev.* 125: 2709–15.

Krishnamurti, T.N., Sinha, M.C., Vasubandhu Misra, and Sharma, O.P. (1997b) "Tropical middle latitude interactions viewed via wave energy flux in the frequency domain", *Dynamics of Atmospheres and Oceans* 27: 383–412.

Krishnamurti, T.N., Bhaskar Jha, Rasch, P.J. and Ramanathan, V. (1997c) "A high resolution global reanalysis highlighting the winter monsoon", *Meteor. Atmos. Phys.* 64: 123–71.

Krishnamurti, T.N., Shina, M.C., Bhaskar Jha and Mohanty,

U.C. (1998a) "A study of south Asian monsoon energetics", *J. Atmos. Sci.* 55: 2530–48.

Krishnamurti, T.N., Bedi, H.S. and Wei Han (1998b) "Organizarion of convection and monsoon forecasrs", *Meteor. Atmos. Phys.* 67: 117–74.

Kuo, H.L. (1965) "On the formation and intensification of tropical cyclones through latent heat release by cumulus convection", *J. Atmos. Sci.* 22: 40–63.

Kuo, H.L. and Qian, Y.F. (1981) "Influence of the Tiberan Plateau on cumulative and diurnal changes of weather and climare in summer", *Mon. Wea. Rev.* 109: 2337–56.

Lau, K.M. and Chan, P.H. (1985) "Aspects of the 40–50 day oscillation during northern winter as inferred from outgoing longwave radiation", *Mon. Wea. Rev.* 113: 1889–909.

Lau, K.M. and Chang, C.P. (1987) "Planetary scale aspects of the winter monsoon and atmospheric tele-connections", in *Monsoon Meteorology*, C.P. Chang and T.N. Krishnamurti (eds), Oxford University Press, Oxford, pp. 3–25.

Laval, K., Raghava, R., Polcher, J., Sadoumy, R. and Forichon, M. (1996) "Simulation of the 1987 and 1988 Indian monsoons using the LMD GCM", *J. Climate* 9: 3357–71.

Levin, Z., Joseph, J.H. and McKler, Y. (1980) "Properties of Sharav (Khamsin) dust; comparison of optical and direct sampling", *J. Atmos. Sci.* 37: 882–91.

Li, C. and Yanai, M. (1996) "The onset and interannual variability of the Asian summer monsoon in relation to land–sea thermal contrasr", *J. of Climate* 9: 358–75.

Lu, M.-M. and Yanai, M. (1987) "Excitation mechanisms of equatorially trapped waves and the tropical low-frequency oscillation during the special observing periods of FGGE", *Preprints, 17th Conference on Hurricanes and Tropical Meteorology*, Miami, Amer. Meteor. Soc., pp. 397–400.

Luo, H. and Yanai, M. (1984) "The large-scale circulation and heat sources over the Tibetan Plateau and surrounding areas during the early summer of 1979. Part II: heat and moisture budgets", *Mon. Wea. Rev.* 112: 966–89.

Madden, R. and Julian, P. (1971) "Detection of a 40-50 day oscillation in the zonal wind", *J. Atmos. Sci.* 28: 702–08.

Magana, V. and Yanai, M. (1992) "Tropical–midlatitude interaction on the time scale of 30 to 60 days during the northern summer of 1979", *J. Climate* 4: 180–201.

Mohalfi, S., Bedi, H.S., Krishnamurti, T.N. and Cocke, S.D. (1998) "Sensitivity of synoptic-scale system and diurnal change to dust aerosols over the Saudi Arabia region", *Mon. Wea. Rev.* 126: 3153–68.

Mohanty, U.C., Iyengar, G.R., Basu, S., Klinker, E., White, G.H., Milton, S.F. and Singh, D. (1994) "An inter-comparison of medium range prediction of selected features of Asian summer monsoon activity with operational GCMs", Proceedings of the Internarional Conference on Monsoon Variability and Prediction, Trieste, Italy, Vol. 1, pp. 351–61.

Murakami, M. (1984) "Analysis of deep convective activity over the western Pacific and Southeast Asia, Part II", *J. Meteor. Soc. Japan* 62: 88–108.

Nakazawa, T. (1988) "Tropical super clusters within intra-seasonal variations over the western Pacific", *J. Meteor. Soc. Japan* 66: 823–39.

Ogura, Y. and Yoshizaki, M. (1988) "Numerical study of orographic connective precipitation over the eastern Arabian Sea and the Ghat mountains during the summer monsoon", *J. Atmos. Sci.* 45: 2097–122.

Palmer, T.N. (1988) "Large-scale tropical, extratropical interactions on time scales of a few days to a season", *Aust. Meteor. Mag.* 36: 107–25.

Palmer, T.N. (1993) "Some thoughts of monsoon predictability", WMO/TD No. 546. Simulation and predictions of monsoons, recenr results, New Dehli, pp. 51–57.

Palmer, T.N., Brankovic, C., Viterbo, P. and Miller, M.J. (1992) "Modeling interannual variations of summer monsoons", *J. Climate* 5: 399–417.

Patterson, E.M., Gillete, D.A. and Stockton, B.H. (1977) "Complex index of refraction between 300 and 700 nm for Saharan aerosols", *J. Geophys. Res.* 82: 3135–61.

Proceedings of the First Internarional AMIP Scientific Conference (1995) WCRP-92, WMO ITD-No. 732, ed. by W.L. Gates.

Ramage, C.S. (1971) *Monsoon Meteorology*, Academic Press, New York.

Rao, Y.P. (1976) "The southwest monsoon", Indian Meteorological Department Monograph, Synoptic Meteorology, 1, Indian Meteorological Department, New Delhi.

Rasmussen, E.M. and Carpenter, T.H. (1982) "Variation in the rropical sea surface temperature and surface wind field associated with rhe Southern Oscillarion/El Niño", *Mon. Wea. Rev.* 110: 345–85.

Rasmussen, E.M. and Carpenter, T.H. (1983) "The relation berween eastern equatorial Pacific sea surface temperatures and rainfall over India and Sri Lanka", *Mon. Wea. Rev.* 111: 517–28.

Shukla, J. and Paolino, D.A. (1983) "The Southern Oscillation and longrange forecasting of the summer monsoon over India", *Mon. Wea. Rev.* 111: 1830–37.

Sikka, D.R. and Gadgil, S. (1980) "On the maximum cloud zone and the ITCZ over Indian longitures during the southwest monsoon", *Mon. Wea. Rev.* 108: 1840–53.

Singh, S.V. and Kripalani, R.H. (1985) "The south to north progression of rainfall anomalies across India during the summer monsoon season", *Pure Appl. Geophys.* 123: 624–37.

Singh, S.V. and Kripalani, R.H. (1986) "Application of EEOF analysis to interrelationships and sequential evolution of monsoon fields", *Mon. Wea. Rev.* 114: 1683–710.

Smith, R.B. and Lin, Y.L. (1983) "Orographic rain on the western Ghat", Proc., First Sino-American Workshop on Mountain Meteorology, E.R. Reiter, Z. Bazhen and Q. Yongfu (eds), pp. 71–94.

Sokolok, I.N. and Golitsyn, G.S. (1993) "Investigation of optical and radiative properties of dust aerosol", *J. Atmos. Environ.* 27A: 2509–17.

Verma, R.K., Subramanian, K. and Dugan, S.S. (1985) "Interannual and long-term variability of the summer monsoon and possible link with Northern Hemispheric surface air temperature", *Proc. Indian Acad. Sci (Earth Planet Sci.) 94* 3: 187–98.

Vernekar, A.D., Zhou, J. and Shukla, J. (1995) "The effect of Eurasian snow cover on the Indian monsoon", *J. Climate* 8: 248–66.

Wang, B. and Xie, X. (1997) "A model for the boreal summer intraseasonal oscillation", *J. Atmos. Sci.* 54 72–86.

Webster, P.J. and Zhang, C. (1989) "Effects of zonal flows on equatorial trapped waves", *J. Atmos. Sci.* 46: 3632–52.

Weickmann, K.M., Lussky, G.R. and Kutzbach, J.E. (1985) "Intraseasonal (30-60 day) fluctuations of outgoing longwave radiation and 250-mb streamfunction during northern winter", *Mon. Wea. Rev.* 113: 941–61.

Yanai, M., Esbensen, S. and Chu, J.H. (1973) "Determination of bulk properties of tropical cloud clusters from large-scale heat and moisture budgets", *J. Atmos. Sci.* 30: 611–27.

Yasunari, T. (1981) "Structure of an Indian summer monsoon system with around 40-day period", *J. Meteor. Soc. Japan.* 59: 336–54.

Zhang, Z. and Krishnamurti, T.N. (1996) "A generalization of Gill's heat-induced tropical circulation", *J. Atmos Sci.* 53: 1045–52.